Programmed and self-organized flow of information during morphogenesis

Claudio Collinet, Thomas Lecuit

Deterministic and self-organizational modes of morphogenetic information

Claudio Collinet[1] & Thomas Lecuit[1,2]

1. Aix Marseille Université & CNRS, IBDM - UMR7288 & Turing Centre for Living Systems Campus de Luminy Case 907, 13288, Marseille, France
2. Collège de France, 11 Place Marcelin Berthelot, Paris, France

Abstract

How the shape of embryos and organs emerges during development is a fundamental question that has fascinated scientists for centuries. Tissue dynamics arises from a small set of cell behaviours, including shape changes, contact remodelling, cell migration, division and extrusion. These behaviours require control over cell mechanics, namely active stresses associated with protrusive, contractile and adhesive forces, and hydrostatic pressure, as well as material properties of cells that dictate how cells respond to active stresses. In this Review, we address how cell mechanics and the associated cell behaviours are robustly organised in space and time to drive tissue morphogenesis. We first outline how not only genetic and biochemical information, but also mechanics and geometry define the time and length scales of the cell behaviours driving morphogenesis. Next, we present two idealized modes of information flow during morphogenesis. The first, akin to a program, follows deterministic rules and is hierarchical. The second follows the principles of self-organisation that rests on statistical rules, local interactions and feedback. As we review the mechanisms of four very general classes of tissue deformations, namely tissue folding and invagination, tissue flow and extension, tissue hollowing and finally tissue branching we delineate the features that fall under either of those two schemes. We suggest a conceptual framework for morphogenetic information that extends significantly from the traditional notion that genes encode shape and that encapsulates genetics and biochemistry as well as mechanics and geometry.

Introduction

The making of an embryo entails the production of billions of cells from one, the fertilised egg, and their organisation into tissues that gradually change shape. This process, known as morphogenesis, consists of characteristic patterns of three-dimensional deformations occurring in specific sequences. The high reproducibility of the shapes produced during embryogenesis argues that tissue remodelling is tightly controlled in space and time and that some sort of information is produced, read and interpreted by cells in the embryo to organise their behaviour. The concentration of specific biomolecules, the rigidity and the shape of the substrate where cells are located and the mechanical forces they are subjected to are few examples of the kind of input cells interpret to define their specific behaviour. This information also ensures that tissue shapes persists in spite the constant renewal of the building components. While molecules and cells turn over within minutes or days, tissue shapes remain stable over days and months. This Review aims at defining the nature of this morphogenetic information and explains the modalities of its deployment during development.

Morphogenesis involves a stereotypical set of fundamental processes driven by cell mechanics that combined give rise to a multitude of tissue and organism shapes. These include: (1) bending or invagination, which generate tissue out-of-plane deformations, (2) tissue flow and extension, which include planar expansion and rotational flows (3) hollowing, i.e. the formation of internal fluid-filled lumens within a tissue, and (4) tissue branching, giving rise to 3D arborisation. In all cases, cells change shape, divide and move with respect to one another. All these processes require mechanical forces, such as tension through contraction of actomyosin networks, cell-cell and cell-substrate adhesion, cell protrusive forces or cell growth. These active forces must be organized in space and time to correctly orient and execute morphogenetic processes. Thus, the primary role of morphogenetic information is to orchestrate cellular mechanics.

The quest to identify the nature of morphogenetic information has fascinated scientists for centuries but has evolved slowly. Key findings from the early 20th century up to the 1990s led to the emergence of the idea that morphogenetic information is encoded by genes which direct developmental processes as a hard-wired program. Development was seen as a sequence of cellular decisions, a "cellular automaton", leading to the differentiation of different cell types occurring on a developmental landscape sculpted by genes[1,2]. Genes defined the developmental trajectories of each cell. This deterministic view has roots in Roux's "mosaic" theory of development[3,4] (Box1) where the fate of cells in an embryo is pre-specified very early on and follows fixed developmental trajectories. The description of stereotyped lineage trees in *C. elegans*[5,6] and Urochordates[7], where genetic determinants segregate at each cellular division defining different cell populations in the progeny consolidated this view. The idea of a genetic program controlling development also has roots in the identification of "morphogens", molecules that determine the positional information within a field of cells via their local concentration. Likewise, genes acting as 'selectors' interpret this positional information, transmit it to the progeny and drive morphogenesis by controlling a battery of downstream 'realisator' genes[8,9]. The discovery of so-called 'master genes', whose simple expression is sufficient to direct the entire genetic program to form an organ, exemplified this view. Remarkable examples of this are *eyeless* and *shavenbaby* in *Drosophila*[10-12] which direct the formation of the eye and larval denticles respectively. Thus, a long tradition substantiated the notion that morphogenetic information is chiefly genetic in nature, and operates as a deterministic program.

However, a number of observations contrasted with this central idea suggesting that development could not possibly result from simple deterministic rules. Already in the late 19th century Driesh and Morgan showed that when sea urchin and amphibian embryos were cut in half, they could re-wire development to regenerate the missing part[4,13-15]. They indicated that during development cells could interact with each other and their environment and adopt a particular fate in a manner that is not pre-determined. Similarly, the seminal grafting experiments in Hydra[16] and amphibian eggs[16,17], showed that certain groups of cells could 'stimulate' the fate of neighbours present in a so-called "competent" state. Thus, development must also result from local cell-cell interactions occurring within the embryo in a self-regulated manner, and proceed by selection of a few viable dynamical cellular states. This so called

'regulative' view of development (Box1) contrasted with the 'mosaic' theory of Roux back in the 19th century. As we will see, both deterministic programs and self-organization underlie the mechanical aspects of morphogenesis[18-20].

In this Review we consider a concept of morphogenetic information that encapsulates not only genetic and biochemical activities but also mechanics and the geometry of cells and tissues. We delineate two idealized modalities of information deployment: one where morphogenetic processes are specified and executed deterministically like a program and the other where the emergences of tissue shape rests on statistical rules, local interactions and feedback following the principles of self-organization. We then discuss how these two modes of information flow manifest in four broad classes of tissue deformations, namely invagination, extension, hollowing and branching.

The nature and flow of morphogenetic information

Changing tissue shape requires control over cell shape (governed by contractility and adhesion), cell movement, cell growth and division as well as cell death. These cell behaviours may be confined to specific regions of tissues, oriented along a given axis, and temporally organised in a sequence or a cycle. Biochemistry, mechanics and geometry are three different modules of morphogenetic information that defines the length- and time-scales of the molecular, cellular and tissue level processes driving tissue shape changes. The way information flows across these modules defines whether morphogenesis is executed like a program or is self-organized.

- **Mechano-chemical and geometrical inputs define time- and length-scales**

Morphogenesis entails that molecular interactions acting at the nanometre scale propagate their activities over many orders of magnitude to specify macroscopic patterns. To this end, length- and time-scales are built internally to organise molecular processes within cells, and cell behaviours within tissues and embryos. Biochemical interactions can define such length- and time-scales (Fig.1A). The rates of chemical reactions tune how quickly specific molecules are produced or degraded, thus regulating their local concentration. When coupled to diffusion, striking spatial-temporal patterns emerge. Reaction-diffusion systems **[G]** such as Turing instabilities **[G]** produce patterns with length-scales that depend on the details of activator-inhibitor interactions[21] (Box2). Excitable systems **[G]** manifest characteristic temporal dynamics, where for instance trigger wave velocities depend on diffusion and positive feedback time-scales[22]. Concentration gradients of molecules where the local concentration depends on the production/degradation rates and on the diffusion/transport constants[23], define time- and length-scales of morphogenetic fields. The emergent biochemical patterns are read and interpreted by cells via cell signalling and direct a sequence of downstream cellular decisions. For instance, the concentration-dependent activity of morphogens transforms a homogenous field of cells into discrete regions of defined length, each with their own morphogenetic and differentiation programs[24,25]. Turing instabilities control palate ridges[26] and digit number in growing limbs[27] in the mouse. Kinetics of transcription factor activation/accumulation can be used to generate temporal patterns of gene expression defining when and in which sequence specific morphogenetic operations occur, as illustrated in the vertebrate segmentation clock[28]. Finally, directional information (e.g. apical to basal, anterior to posterior, etc.), can come from the polarized accumulation of specific molecules in cells. Thus, scalar information (i.e. the concentration of a molecule) can produce vectorial or tensorial information, namely the orientation of cell polarity, cell shape and dynamics.

Mechanical parameters such as elasticity, viscosity and friction can also specify time- and length-scales (Fig.1A). For instance, the length-scale of stress propagation, the so-called hydrodynamic length, depends on the relative contribution of viscosity and friction within a cell[29] or a tissue. Viscosity can also define rates of deformation upon a given mechanical stress. The ratio between the viscous modulus and elastic modulus defines the Maxwell time, i.e. the time above which deformations become irreversible, typical of a viscous response **[G]**[30]. Mechanics can direct morphogenesis in a manner similar to biochemical information. For instance, dissipation of a localized stress by friction can generate gradients of stress similar to those better known for morphogens[31,32]. Turing-like mechanical instabilities

produce cellular patterns with length-scales governed by the elastic resistance of the extracellular matrix to active stresses produced by motile cells as in the case of feather bud morphogenesis[33,34] (Box 2). Subcellular patterns of actin assembly also emerge from the frictional resistance to actomyosin active hydrodynamic flow[35] (Box 2). The length scales are tuned by the competition between a local positive mechanical feedback and a long-range inhibition (elasticity or friction). Mechanosensation and mechanotransdution, by specialized cellular structures such as tight and adherens junctions[36-39] as well as focal adhesions[38,40,41] can elicit specific signalling driving cell behaviours[42]. Mechanical stresses can also vary in direction (e.g. isotropic or anisotropic) or in nature (e.g. tensile versus shear stresses) and thus can define the type and direction of cell and tissue deformations.

Morphogenetic information thus is both chemical and mechanical and often exhibits hallmarks of mechano-chemical coupling[19,43]. Thus, the interplay between biochemical reactions and mechanical processes enriches how length- and time-scales may be defined. For instance, positive and negative regulators of mechanics (e.g. active stress dependent on MyoII activation) may be advected[44,45] or recruited[46] by contractile actin filament networks (Fig.1A) or specific signalling may be elicited through mechanotransduction.

Both biochemical and mechanical information operate in an environment that is defined by the geometrical configuration of the tissue, namely its dimensionality, size and curvature. These factors constrain how biochemical and mechanical activities are deployed in space and time. Geometry enables non-local coupling between different parts of a cell, tissue or embryo, and defines boundary conditions **[G]** dictating how stress is distributed within a tissue[32]. This has important consequences in the way mechano-chemical information affects the cellular processes driving morphogenesis. For instance, polarized cell intercalation drives linear tissue extension or rotation depending on whether tissue boundaries and the axis of polarisation are linear or circular. Tissue bending modulates concentration gradients of morphogens[18,47,48]. Thus, tissue geometry contains information that complements and interacts with mechano-chemical information during morphogenesis.

- **Morphogenetic information flow: program versus self-organization**

We present two idealized modes of information flow: one in which morphogenesis is carried out as a program and another in which it is self-organized (Fig.1B). These modes represent two ends of a continuum spectrum that often co-exist in a given process.

In ‘programmed morphogenesis’ information is prescribed by a set of initial conditions (e.g. genetic/biochemical patterning and/or initial geometry) and determines fully the mechanical behaviour of cells (e.g. distribution of active stresses), the number, amplitude, location and time of morphogenetic processes and the final shape. Thus, the initial information, which is visible as an inherited prepattern such as a chemical gradient, foretells the final outcome of the morphogenetic process. A strict hierarchy, a unidirectional flow of information and deterministic rules are characteristic features of a morphogenetic program. The interactions between the players of morphogenesis can be direct or indirect, i.e. mediated by intermediate layers of controllers and effectors, organised in functional units (e.g. cell division, cell contraction). For instance, patterning cues might control the expression of a ‘master gene’ (e.g. *shavenbaby*), the activation of intermediate regulators and effector molecules (e.g. actin nucleators, cuticle synthesis enzymes) to determine a specific cell behaviour (e.g. denticles **[G]** formation)[12].

In contrast, in ‘self-organized morphogenesis’ the initial state is homogeneous and does not foretell the final outcome of morphogenesis. Shapes emerge from an apparently disordered state associated with stochastic fluctuations. Amplification of local fluctuations through feedback and spatial coupling let the system evolve towards an organised steady-state. Self-organisation is characterized by the absence of a hierarchy between information modules and by multidirectional flows of information. Biochemistry, mechanics and global geometry influence each other, forming a constantly updated information that drives tissue shape changes. Thus, mechanics and the evolving shape (geometry) of the tissue are part of the information itself and not just under its control. This is exemplified by the processes of morphogen gradient bending in the chick intestinal villi[48] or luminal signalling in the Zebrafish migrating lateral line primordium[47] where tissue mechanics and morphogenesis remodel morphogen gradients and tissue

patterning. The bending of the intestinal epithelium during villification, concentrates an otherwise uniform distribution of Sonic Hedgehog (Shh) at the tip of villi, thus restricting the specification of progenitors to the crypts[48]. In the Zebrafish lateral line, rosette formation due to contractility-dependent apical constriction restricts a source of secreted FGF into a shared microlumen where FGF concentrates and activates downstream target genes[47].

Tissue bending, folding and invagination

Curving and bending tissues lead either to the formation of stable folds or to complete tissue invagination. During embryogenesis, single tissues invaginate to produce independent tissues such as the neurectoderm, which gives rise to the neural tube, the mesoderm, to muscle tissues, and the endoderm, to many internal organs (e.g. gut). Adult organs are also often folded (e.g. brain). Folding and invagination may occur at very specific locations and defined steps determined genetically. Folding may also display features of self-organisation, that is, arise at locations without strictly defined cue. Tissue-intrinsic active stresses, such as actomyosin contractions or tissue growth together with external stresses, stemming from the geometrical configuration of the tissue and its boundaries drive bending and folding.

- **Contractility-driven invaginations**

Tight control over tissue bending and invagination occurs during embryonic gastrulation as it is essential that the different germ layers be properly configured in 3D. A general strategy is the constriction of the apical surface of epithelial cells followed by contraction of lateral surfaces and basal expansion (Fig.2A). Controlling the geometry of the domain where cells change their 3D shape and their timing determines precisely where and when invaginations occur in the embryo. This is determined by genetic patterning and typically follows the principles of a morphogenetic program.

The mechanics of contractility-driven tissue invaginations have been thoroughly studied in *Drosophila* where the invagination of the mesoderm illustrates how cell contractions drive invaginations as a program[18,49,50]. Along the ventral side of the fly embryo a band of cells forms a furrow and internalizes (Fig.2B)[51,52]. Pulsed contractions of an actomyosin network at the medio-apical cortex of mesodermal cells drives their apical constriction[53] and cell lengthening along their apico-basal axis[54] in discrete steps[49,50,53]. Then, cells expand their basal surface via local downregulation of actomyosin contractility[55], and lateral contractility facilitates invagination[56]. Similarly, during endoderm invagination of the urochordate *Ciona intestinalis* cells first induce apical constriction by apical activation of MyoII, followed by lateral cell shortening also requiring MyoII contractility[57]. Thus, polarized regulation of apical, lateral and basal actomyosin contractions underlies stepwise cell deformation during tissue invagination. The extent and sequence of spatially controlled cell contractions determine the complex morphology of the invagination[57].

Spatial and temporal control of actomyosin contractility follows the principles of a genetic program in the *Drosophila* mesoderm. Here the small GTPase Rho1 (homolog of RhoA in mammals), through activation of the kinase Rok (called ROCK in mammals), controls MyoII contractility[58,59] (Fig.2C). Rho1 activation is necessary and sufficient to elicit apical constriction and tissue invagination[60]. The spatial and temporal pattern of Rho1 activation defines the pattern of tissue invagination[60]. In the *Drosophila* embryo the expression of the transcription factors Twist and Snail, who in turn depend on the DV gradient of Dorsal[61], patterns Rho1 activation and MyoII contractility (Fig.2B-C). Twist and Snail drive the expression of the G-protein-coupled-receptor Mist[62], its secreted ligand Folded gastrulation (Fog)[63], and the transmembrane protein T48[64] that boosts recruitment RhoGEF2 apically where it activates Rho1. Thus, *twist* and *snail* form a 'genetic switch' and drive tissue invagination as a program, receiving input from developmental patterning and controlling the cellular effectors of the program.

Similarly, in *C. elegans* contractions of a medio-apical actomyosin network drive apical constriction and invagination of the two endoderm precursor cells[65,66]. The specific and polarized activation of MyoII in these cells is controlled by the Wnt-Frizzled signalling pathway[65] and two endoderm specific

transcription factors, END-1 and END-3[67]. In vertebrates, apical constriction drives tissue bending during the neural tube closure in several organisms[68,69], gut morphogenesis in *Xenopus*[70] and the eye lens placode invagination in the mouse[71,72]. The conserved RhoA/ROCK/MyoII module, together with other actin regulators (Mena **[G]** /VASP **[G]**), tune the contractile forces driving apical constriction. The proper spatial and temporal activation of this module is controlled by genetic patterning through tissue-specific expression of the Shroom family proteins **[G]**[70,71,73]. These proteins bind apical cell-cell junctions[74,75] and direct MyoII activation through their direct binding to ROCK.
Altogether, these findings highlight how tissue invaginations can be directed by tissue-specific genetic programs that determine the spatial and temporal patterns of MyoII activation, and subcellular polarization. Nevertheless, this conceptual framework fails to explain all features of contractility-driven invaginations. First, the pulsed actomyosin contractions driving invagination, which are a common feature observed in many developmental contexts[66,76-80], are not specified genetically but rather depend on [44,46,58,59]self-organizing properties of actomyosin networks[44] due to their association to upstream regulators of MyoII contractility[44,46,58,59]. Second, tissue-level properties such as spatial coordination of contractions[81] and the robustness of the invagination[82] are emergent properties of the cell collective. Third, the emergent mechanical properties of a supracellular actomyosin networks can in some cells override the genetic program driving apical constriction in their neighbors[83].
Self-organizational features of contractility-driven invaginations can also manifest in the dynamics of the invagination process, that is, how the tissue reaches its final shape from a specified initial pattern. In some cases, the final shape greatly diverges and cannot be predicted from the pattern of the triggering input. This was shown using modelled epithelia[84] where tissue invaginations of different shapes arise by apical constriction in a self-organized fashion using a single cell as trigger. The model, based on an excitable apical cortex which induced cell contraction upon cell stretching above a given threshold, predicted waves of apical constriction initiating from single contracting 'triggering' cell[84]. Tuning of mechanical parameters produced a variety of configurations observed in invaginating tissues *in vivo*. A similar induction and self-propagation of a wave of MyoII contractility driving cell invagination occurs in the *Drosophil*a endoderm (Fig.2D-E)[42]. An initial phase of MyoII activation, apical constriction and tissue invagination is triggered in a spatially defined region at the embryo posterior, controlled by a genetic program similar to that of the mesoderm. The expression and secretion of the "switch factor" Fog, under the control of terminal patterning[63], define the region of initial invagination and triggers MyoII activation. Subsequently, MyoII activation and cell invagination propagate anteriorly driving the movements of the endoderm towards the embryo anterior. The associated morphogenetic wave does not depend on a wave of gene transcription nor on the regulated diffusion/transport of secreted signals such as Fog activating MyoII. Rather the wave is controlled mechano-chemically by self-sustained repeated cycles of cell deformations involving adhesion to the overlaying vitelline membrane **[G]**, which forms a substratum to direct tissue movements and activate MyoII through integrin mechano-chemical signalling[42]. Thus, dynamic patterns of tissue invagination can arise from the interplay between a genetic program that works as a trigger and self-organised mechano-chemical propagation.

- **Folding by growth-driven mechanical instabilities**

Some tissues consist of many folds organised in complex patterns, such as convolutions in the brain and looping and villosities in the gut. These folds arise in sheet- or a rod-like tissues due to mechanical instabilities associated with tissue growth. An elastic material put under compressive forces folds to relax stresses above a certain threshold. Likewise, the planar growth of a tissue generates compressive stresses when the increase in size is constrained, for instance when the neighbouring tissues do not grow as fast (Fig.3A). Thus, differential growth leads to folding or looping. Notably, in the absence of other cues, the final pattern of folding and looping is not strictly determined but self-organised, in that the position and amplitude of folds and loops follows stochastic rules. This typically occurs in the brain folding of gyrencephalic species[85,86] and gut morphogenesis[87,88].

The brain cortex in vertebrates is characterized by a complex folding pattern with outward (gyri) and inward curvatures (sulci) (Fig.3B). In the mature cortex these folds are evenly spaced. Brain circumvolutions form progressively on an initially smooth morphology[89,90], starting with the emergence of few 'primary' sulci at stereotyped locations[91,92]. Then other folds form with a lower degree of

stereotypy[89]. Across different species, the extent of cortical folding scales as a function of cortical surface area and its thickness in a manner similar to the crumpling of paper balls[93], suggesting that brain folding may follow principles of energy minimization[93]. Although several models have been proposed[94,95], the source of stresses associated with folding appears to be an difference in tangential expansion between the external (grey matter) and internal (white matter) layers of the brain cortex. This hypothesis[96] was consistent with theoretical studies in several contexts[97-99], and received support from measurements of physical forces in developing ferrets brains[100] and more recently, from experimental testing with synthetic 'mini brains'[101,102]. Using 3D gels with controlled stiffness and computer simulations it was shown that greater swelling of the outermost layer compared to the inner core produced a wrinkling pattern with smooth gyri and cusped sulci similar to that observed in brain cortices (Fig.3C)[101]. Furthermore, when the size and the shape of gel and *in silico* 'mini brains' were made similar to the geometry of foetal human brains before cortical folding, the pattern of gyri and sulci was remarkably similar to that observed *in vivo*[102]. The non-uniform local curvature in the smooth template determined the spatial distribution of stresses, with highest compressive stresses at sites of *primary* sulci formation, which were remarkably similar to the positions found in real brains by *in utero* MRI[102]. These findings highlight how mechanical instability and the initial foetal brain geometry could generate reproducible folding patterns. However, it was proposed that additional information is necessary to control the stereotyped folding pattern of primary sulci *in vivo*. Patterned local heterogeneities in the thickness of the subventricular zone (a region of high neurogenesis in gyrencephalic species) and the proliferation of radial cortical progenitors correlate with the position of emergence of gyri and sulci[103-105]. A transcriptomics analysis in ferret brains identified specific modules of gene expression mapping the prospective positions of primary fissures[106], supporting the idea that regional differences in growth might be genetically encoded. The information required to position primary fissures thus supports the existence of an underlying folding program.
Brain folding is thus an example of morphogenesis emerging from the mutual interactions between patterning (differential growth), tissue mechanics (elasticity) and tissue geometry.

Another context where growth-driven mechanical instabilities drive morphogenesis is the development of the gut which undergoes looping and vilification as it extends. Throughout development, the growing gut tube is attached to the dorsal mesentery, a type of membrane connecting the body to the gut tube along its entire length (Fig.3D). Upon physical separation from one another these two tissues recoil: the tube unwinds and the dorsal mesentery shrinks, indicating that the former is compressed while the latter stretched[107]. In their relaxed state the two tissues have different sizes reflecting their different growth. Thus, gut looping results from buckling to relax the stress accumulating when the tissues are physically attached to one another and grow at different rates as shown using a simulacrum connecting two elastic materials of different lengths (Fig.3E) and by computational modelling[107]. Bmp signalling, present in a dorsal to ventral gradient from the dorsal mesentery to the mesenchyme of the gut tube[108], tunes the extent of differential growth and as result the degree of gut looping[109], but the specific position of loops emerges stochastically. Thus, the degree of looping can be seen as encoded in a program but the looping pattern is self-organized.
In many species the gut undergoes villification which transforms its luminal surface from flat to convoluted with the emergence of numerous inward protrusions such as ridges, zig-zags, honeycombs and villi. The hypothesis that these structures might arise from the constrained growth of inner layers by outer contractile muscle cells was formulated long ago[110] and recently tested[98,111]. In the chick, this process is well characterized and occurs at discrete steps: first longitudinal ridges form; then they fold in a zig-zag pattern and finally villi form (Fig.3F)[110,112,113]. This tightly follows the formation of first circumferential muscles, followed by 2 separate layers of longitudinal muscles. These muscles mechanically constrain the growth of the internal layers: circumferential muscle contraction induces longitudinal ridge formation, while longitudinal muscle contraction induces lateral buckling of ridges into zigzags[111]. The last step involves inhomogeneous growth of the intestinal epithelium where growth is confined to the valleys between forming villi[111]. Interestingly, this final pattern emerges from the continually changing geometry of the tissue during the formation of villi, which bends a gradient of the Shh and leads to the formation of a signalling centre at the villi tip, ultimately restricting cell proliferation at the base of villi[48]. Thus, in the chick vilification emerges from growth-mediated mechanical instabilities (self-organization) acting upon patterned mechanical constraints (program).

Vilification in the mouse, is apparently not constrained mechanically and may depend rather on chemical (e.g. Turing) instabilities[114,115]. Self-organised patterns of BMP2 induce mesenchymal condensates prior to villi formation. Although this can be modelled as a Turing instability, it is conceivable that mechanics also participates in the formation of such self-organised condensates as postulated[116] and subsequently tested for the morphogenesis of feather buds[34] (Box.2). Mechano-chemical instabilities could therefore be a general framework for thinking about vilification across species where similar coupling of smooth muscle layer differentiation and folding of internal layers have been observed.
Gut morphogenesis exemplifies how complex shapes emerge from stresses due to differential growth, tissue elasticity and tissue geometry.

Tissue flow and extension

Tissue flow is commonly observed during morphogenesis and is associated with tissue extension or rotation. Extension is a widespread rearrangement whereby a tissue lengthens in a preferential direction and is driven by active cellular processes such as cell rearrangements. Interactions with boundaries, which can be fixed or moving, provide additional extrinsic forces and/or orient the flow due to intrinsic stresses in a preferred direction (Fig.5A-A'''').

- **Programmed polarization of cellular active stresses**

Cell intercalation by convergent-extension **[G]** movements often drive tissue extension (Fig.4A). Historically, two distinct modes of cell intercalation have been described in mesenchymal and epithelial cells[117,118]. However, more recent evidence indicates that these two modalities can coexist in the same cells and contribute to the local active forces driving tissue flow[119].

A first mode of intercalation is by cell motility whereby cells extend polarized actin-rich membrane protrusions and intercalate by displaying movements typical of migrating cells. This mode was described early on in cells of the dorsal mesoderm and of the overlying neural plate during gastrulation and neurulation in the frog embryo[120-122]. These cells extend bipolar actin-rich lamellipodia along the medio-lateral axis of the embryo (Fig.4B) that make stable contacts with and exert traction forces on neighbouring cells[79,123-125]. In the ascidian notochord **[G]**, epithelial cells intercalate medio-laterally in a process that depends on the polarized membrane protrusions along their apico-basal axis[126]. During formation of the dorsal midline in *C. elegans,* polarized Rac-dependent membrane protrusions at the basolateral side of two rows of cells drive their migration and intercalation in the embryo midline[126-128].
The polarized extension of actin-rich protrusion at the basolateral side of epithelial cells occurs together with remodelling of cell-cell junctions and contributes to the formation of rosettes in the germband **[G]** of *Drosophila*[129] and in the mouse neural plate[130].
The second mode of cell intercalation is by polarized remodelling of cell-cell contacts via actomyosin contractions. Cells exchange neighbour while maintaining intercellular adhesion and tissue integrity (Fig.4D). This mode was first characterized in epithelial cells of the germband in *Drosophila*[131] where dorsal-ventral (DV)-junctions first shrink and then new antero-posterior (AP)-junctions form[132,133], thus extending the tissue along the AP axis. Planar polarized actomyosin contractility at cell-cell junctions[132,133] and in the medio-apical cortex[76,134-136] drive junction remodelling. Junctional MyoII accumulates at DV-junctions[132,133] and induces anisotropic cortical tension[137-140] while medial MyoII undergoes planar polarized flows that increase the speed of shrinkage of DV-junctions[76,134] and extend new AP-junctions[135,136]. Similar junction remodelling by actomyosin contractions drive cell intercalation in vertebrates, such as during primitive streak **[G]** formation[141] and neural tube closure in chick embryos[68,142]. Remarkably, mesenchymal cells of the dorsal marginal zone **[G]** in frog embryos present similarities with the epithelial cells of the *Drosophila* germband[143,144]. Phosphorylated MyoII accumulates at mediolateral cell-cell contacts inducing anisotropic cortical tension[143] and actomyosin pulses correlate with steps of cell-cell contact shrinkage[143,144].
Thus, the extension of actin-rich membrane protrusion and remodelling of cell-cell contacts by actomyosin contraction are complementary strategies to produce local active forces required for cell intercalation.

Global tissue polarity must be transmitted locally to orient the active cell processes driving extension. In *Drosophila* embryos the global polarity encoded in the gradients of the anterior and posterior determinants Bicoid and Caudal, is transformed in the striped expression of pair-rule genes **[G]**, in particular *even-skipped* (*eve*), which in turn controls planar polarization of MyoII[145] and cell intercalation (Fig.4E)[131]. The polarization of MyoII by *eve* is mediated by three Toll receptors **[G]** expressed in a specific striped pattern repeated in each parasegment[146]. The differential expression of Toll receptors between neighbouring rows of cells is thought to activate MyoII at DV-junctions[146,147]. How Toll receptors activate MyoII at junctions is not yet clear. Tolls may polarize GPCRs activity that regulate Rho1 and MyoII activation. Recent evidence indicates that the adhesion GPCR Cirl/Latrophilin forms a complex with Toll8 that mediates MyoII polarization[147]. However, Toll8 and Cirl polarization are dynamically interdepended when neighbouring cells express different levels of Toll8[147], indicating that the mechanism of receptor polarization itself occurs through self-organization.
Another pathway that translates global directional information locally to cells is Planar Cell Polarity **[G]** (PCP) signalling (see[148-150] for excellent reviews). Interestingly, PCP signalling polarizes cells acting, amongst others, on Rho and Rac signalling[117,151-154]. and controls polarized cell intercalation in many mesenchymal[155,156] and epithelial[130,142,157] systems. In the frog, interfering with PCP signalling disrupts both the bipolar extension of actin-rich protrusions[156] and the contractions of medio-lateral shrinking cell-cell contacts[143]. The precise mechanism is not yet clear. PCP proteins, which localize at medio-lateral cell-cell contacts[158], might polarize cells by promoting Rho signalling and MyoII activation at these contacts[159], thus also restricting Rac and protrusive activity medio-laterally (Fig.4C). Septins **[G]**, which act as diffusion barriers and regulate medio-lateral intercalation downstream of PCP[143,160], might mediate this polarized partitioning. In epithelia, PCP signalling controls directed cell intercalation in several contexts: it orients cell intercalation in the ascidian notochord primordium[157], it polarizes both the extension of basal protrusions and apical junctional remodelling in the mouse neural plate[130] and it controls polarized MyoII activation at adherens junctions in the chick neural tube via activation of the GPCR Celsr1 (Fig.4E)[142]. These examples highlight how global spatial and directional information laid down by genetic patterning is interpreted by different planar polarity systems to control and coordinate local intercalation driving tissue extension. Tissue extension can thus be seen as controlled by a genetic program.

This program view of tissue extension must be nuanced with the fact that local cell dynamics during cell intercalation follow statistical rather than deterministic rules. The most striking stochastic feature is the pulsatile nature actomyosin contractions. In the *Drosophila* germband, actomyosin pulses are self-organised and involve Rho1GTP oscillations entrained mechanically by MyoII-driven advection of Rho1GTP and Rok[44]. Moreover, medio-apical pulses flow towards cell-cell contacts with a statistical bias in the AP-direction[76,161]. Thus, DV-junctions are more likely to shrink also based on statistical considerations. Last, local deformations induced by actomyosin contractions are not strictly irreversible. Only contractions longer than a dissipation time scale produce permanent deformations[30]. This dissipation time functions as a bandpass filter for loosely controlled actomyosin pulses. This ensures global persistent junction remodelling in face of inherently fluctuating cellular dynamics. The reliance on fluctuations is a characteristic feature of self-organisation and underlies tissue extension in the *Drosophila* germband.

- **Self-organization via patterned boundary conditions and external forces**

Tissue flow and extension is not solely driven by polarized internal stresses. The geometry and patterning of tissue boundaries as well as extrinsic forces impact on cellular dynamics and/or orient tissue flows (Fig.5A). Boundary conditions can either exert mechanical feedback on cellular dynamics or simply define geometrical constraints and direct cellular flows. An example of mechanical feedback is again *Drosophila* germband extension. Here the invaginating posterior endoderm is an actively moving tissue boundary (Fig.5C) and exerts a posterior pulling force onto the germband[135,162] that orients the extension of new junctions along the AP-axis[135]. This optimizes the extension process by aligning local junction extension with the global direction of tissue lengthening[135]. Actively moving boundaries organize also large-scale flows associated with primitive streak formation during avian gastrulation[163].

Here the contraction of a supracellular actomyosin ring at the margin of the embryo acts a moving boundary that drives the flows (Fig.5E).

A feedback between extrinsic forces and intrinsic cellular processes occurs also during the morphogenesis of the fly wing. Here a tissue-level contraction of the hinge, the part of the wing connected to thorax, pulls and extends the wing blade along the proximo-distal axis (Fig.5B)[164]. This induces a pattern of cell elongation, cell rearrangements and cell divisions[164,165] which underlies not only tissue extension but also the alignment of PCP components along the proximo-distal axis[164].
Attachment to a fixed substrate controls the orientation of tissue-level forces, ultimately defining the pattern and direction of tissue extension. In the fly wing the pattern of distal attachment of epidermal cells to the overlaying cuticle by the extracellular matrix protein Dumpy directs tissues-level tension and shapes wing extension (Fig.5B)[165,166]. Modifying the pattern of attachment has predictable consequences on the final wing shape indicating that wing morphogenesis results from patterned tissue contraction and localized anchorage[166]. Another context where the attachment to a fixed substrate directs cellular flows is gastrulation of the red flour beetle *Tribolium castaneum*[167]. Here gastrulation consists of the contraction and folding of a large part (approximately two thirds) of the epithelial blastoderm, which gives rise to the future embryo, and the spreading of the remaining third, which gives rise to the enveloping serosa. The flow of the serosa is unidirectional and depends on the localized attachment of the blastoderm to the overlaying vitelline membrane mediated by integrins[167].
Thus, tissue extension is patterned by mechanical coupling at tissue boundaries. These boundaries, whether active or fixed deterministically orient tissue extension and cellular flows. Yet morphogenesis of the system as a whole is self-organizational given that the behaviors of the cells are not individually programmed and mutually interdependent. Strikingly, the geometry of tissue boundaries orients the flow pattern. Given polarized cell intercalation the boundaries may drive rectilinear, curvilinear or rotational flow as illustrated respectively in the *Drosophila* wing, germband and male genitalia[168] (Fig.5A-A’’’). Thus, tissue boundaries carry both mechanical and geometrical information required for tissue extension.

Tissue hollowing and lumen formation

Many organs and embryos change their topology through the formation of a fluid-filled lumens. This process occurs in organs such as the liver canaliculi the otic vesicle or the early mouse embryo and is regulated by mechanics, hydraulics and cell and tissue geometry[169-175].

Fluid-filled lumens form within the extracellular space of simple cell aggregates (Fig.6A) by either apoptosis in the centre of the aggregate or through the polarized secretion of fluid filled vesicles[176,177]. Lumen growth is powered by water flux through cells due to a gradient of osmotic pressure maintained by energy consuming ion pumps driving polarized ion transport inside the lumen[172,178-181]. The hydrostatic pressure within the lumen is resisted by cortical tension in the surrounding tissue[174,176] (Fig.6A). Small lumens are unstable but once they reach a critical size they grow, powered by the osmotic pressure. A negative feedback explains how lumen size reaches a stable steady state or oscillatory dynamics around a fixed size. The spherical nature of the shell is such that surface tension increases as the hydrostatic pressure of the growing lumen increases. Above a threshold value of surface tension and cell stretching cells may leak water through junctions and thereby the lumen shrinks rapidly as documented in organoids and the mouse blastocyst[173,175]. Water flux may also be reduced as internal pressure increases as documented in the zebrafish otic vesicle[182]. Finally, lumen dynamics may depend on competition between active ion transport, water flux, passive ion permeation, cortical tension and leakage through junctions, which depends on the geometry of the cell aggregate as shown for liver canaliculi[174]. Thus, lumen formation and growth are governed by many feedbacks and follow principles of self-organization.

In some cases, lumen formation and growth also control the patterning and size of an organ or an embryo as in the formation and growth of the blastocoel in the mouse embryo. The blastocyst is the mammalian

pre-implantation embryo composed of the trophectoderm (TE), an extraembryonic tissue that envelopes the inner cell mass (ICM) forming the embryo proper, and a fluid-filled lumen termed blastocoel. The blastocoel is positioned invariantly at the interface between TE and the ICM, which clusters on one side, thus breaking the initial radial symmetry of the embryo. This sets the first embryonic axis that later defines the main axis of the mammalian body[183]. Blastocoel formation in mouse embryos[184] begins with the simultaneous accumulation of fluid in hundreds of micron sized lumens in the intercellular space between cell-cell contacts[184] (Fig.6B). A rise in intercellular hydrostatic pressure locally "fractures" E-cadherin cell-cell junctions and forms these microlumens. Since the microlumens are connected, the fluid eventually converges in a single large lumen by flowing from small to large lumens due to pressure differences and periluminal contractility. Patterning cell-cell adhesion and cell contractility orients the fluid flow and define the final position of the blastocoel[184]. While there are no known patterns of cell-cell adhesion molecules in the mouse blastocyst, ICM and TE cells have different cortical tension. Higher contractility in ICM cells drives their initial internalization in the embryo[185,186]. The blastocoel forms at the interface between the highly contractile ICM cells and the softer surrounding TE cells, which maintain a polarized structure with an apical plasma membrane domain at the cell-free interface (Fig.6B). In TE cells the presence of an apical plasma membrane domain reduces acto-myosin contractility[185,187], such that cell contractility depends on cells position within the embryo. Thus, mechanical and geometrical information position the blastocoel and set the first embryonic axis in mouse embryos.

Once formed and positioned the blastocoel keeps accumulating fluid, ultimately enlarging the blastocyst. The swelling of the blastocoel is resisted by tight junctions, which prevent fluid leakage, and by cortical tension of TE cells (Fig.6B). The expansion of the blastocoel stretches TE cells which in turn respond by increasing their contractility and strengthening tight junctions by a mechanical feedback[175]. The blastocyst keeps increasing its size up to a threshold in cortical tension where intermittent collapses are observed due to ruptures of tight junctions when TE cells divide. Thus, feedback between lumen pressure, cell contractility and junction stabilization regulate the size of the embryo in a self-organized manner[175]. Tissue size regulation affects in turn cell fate specification within the embryo. Indeed, decreasing the size of the lumen (thus decreasing outer cells stretching) facilitates internalization of cells possibly by affecting the orientation of outer cell divisions. Since the lack of an apical surface is required to downregulate CDX2[188,189], a TE cell fate determinant, regulation of blastocyst size also impacts on specification of blastocyst cell identities[175]. Furthermore, the expansion of the blastocoel, through a mechanism not yet fully characterized but involving the secretion of FGF-coated vesicles in fluid filled lumen, also patterns the spatial segregation of the epiblast and primitive endoderm **[G]** cells within the ICM[190]. Thus, mechanical and geometrical cues set size and patterning in the blastocyst by shaping cell fate defining biochemical signalling.
Altogether, hydrostatic pressure drives tissue morphogenesis and mechanical as well as geometrical feedback mechanisms control tissue size and patterning. This provides an example of self-organised tissue morphogenesis in the absence of a pre-established genetic program.

Branching morphogenesis

Branched structures are ubiquitous in nature, from molecules, to cells and entire organs. Many internal organs, such as the pulmonary tract, exocrine glands, the kidney and the vascular system have branched structures that are essential for their functions. Excellent reviews[191-193] summarize the known molecular mechanisms of morphogenesis of branched organs; here we illustrate how branching morphogenesis follows the principles of programmed morphogenesis or self-organization.

The *Drosophila* tracheal system is a highly ramified epithelial tubular network that transports oxygen to internal organs. Its branching pattern is highly stereotyped[194] and is driven by sources of FGF[195] as a guidance cue. Tracheal development begins with the invagination of 20 epithelial sacs, each sprouting finer branches to generate a tree-like structure. Sprouting depends on the migratory activity of few epithelial cells towards a localized source of FGF (Branchless)[195]. The expression pattern of the FGF source is not fixed but changes dynamically. Once primary branches reach the source of FGF this is

turned off and branches stop growing. Successively, expression of Branchless at a new location guides branch elongation towards the new patch[195]. Thus, the localized and dynamic expression of a source of FGF signalling controls deterministically the branching pattern, like in a program.
The development of the mouse lung also shows stereotypical patterns akin to a program. The reconstruction of the complete branching history of the pulmonary tree identified 3 unique and geometrically simple modes of branching that form the entire pulmonary tree[196] (Fig.7A). These 3 branching modes do not occur randomly in the lineage but according to only 3 specific sequences (Fig.7A). Thus, like a program, individual modules (the branching modes) are repeated according to deterministic routines (the branching sequences), proposed to be genetically encoded by a 'master routine'[196].

Contrasting with this view it was proposed that the morphogenesis of branched organs (e.g. the mouse mammary gland and kidney) can also emerge from stochastic rules for the branching, elongation and termination of the tips of the network[197] (Fig.7B). Key features of the branched network could be predicted by a model where the branch tips can either bifurcate or elongate in a random direction with equal probability and terminate when they reach the proximity of existing ducts, introducing a density-dependent negative feedback on network growth. In this case the precise shape of the network is not pre-determined genetically but self-organized as it emerges from a space-filling strategy driven by local rules. This model predicted several features of the branched trees in the mouse mammary gland and kidney such as a structural heterogeneity of network subtrees, a constant density of branches. and an in-built polarity of network growth emerging from its design rules without any chemotactic gradient[197] (Fig.7B). This study shows how branching can be self-organized through local interactions and feedbacks. The global network topology and its features are defined by statistical rules of intrinsically noisy cell dynamics.

The dichotomy between program and self-organization is not limited to the branching of internal organs. Neurons too displays features of deterministic and self-organized branching in growing their dendritic arborizations. One context where deterministic rules fully determine the arborization pattern are the dendrites of the PVD neurons in *C.elegans*. Very stereotypical dendrites arborizations are established in PVD neurons during postembryonic development[198,199] and are dependent on patterned cues provided in the epidermis[200-202]. Here the ligand complex SAX-7/L1CAM/MNR-1 expressed in the skin controls the growth of ''menorah''-like dendrites by acting as a short-range cue for branching points[200,201]. In *Drosophila* vdpa class-I neurons the shape of the dendritic arborization are defined by a combination of deterministic rules and self-organization (Fig.7C). In these neurons the growth of the primary branch occurs very robustly in a pre-determined direction while the secondary and tertiary branch display fluctuations in length and number characteristic of stochastic systems[203]. Live imaging of dendritic growth and computational modelling revealed that the shape of the neuronal arborisation emerges from few local statistical rules of branch dynamics. Moreover, the tree geometry exerts a constant feedback on local branch dynamics in two opposite ways: branch stabilization by child branches and contact-induced self-repulsion of internal branches[203]. Thus, the morphogenesis of complex branched dendritic arborizations relies on both deterministic and self-organizational principles.

Conclusions and perspectives

How are biological forms encoded? The information that underlies morphogenesis is inherited genetically. Though genes somehow specify via their biochemical products how their activities are organised in space and time, they do not do it explicitly, and it is essential to consider the physical environment in which they operate. Understanding how genes encode shape requires a characterization of fundamental physical properties of living matter that are not genetically encoded. Such properties can be encapsulated in theory: for instance, the law of diffusion, the theory of linear elasticity, active matter theory, that explain how dynamics emerge from local out-of-equilibrium properties of molecules or cells. Biochemistry and mechanics both define length-scales and time-scales and as such underlie how shapes emerge. Morphogenetic information is thus inherently mechano-chemical.

However, morphogenetic information is also geometrical. Geometry of a tissue defines the systems boundary conditions, impacts on local stress patterns and can reshape chemical gradients. This has profound consequences on how mechanochemical information is deployed in space and time. While geometry is an essential information during morphogenesis, cells cannot directly sense their shape *per se*, but only via stresses and biochemical activities that arise from geometry. Importantly, shapes can emerge from mechano-chemical information, so geometry may feedback and update local molecular activity and local mechanics. As such, the morphogenetic information is recursive as it acts upon itself and updates constantly through feedback.

We delineated two idealised and distinct modalities of information flow during morphogenesis. Programs specify deterministically and hierarchically all operations required for the development of a shape. Programmed morphogenesis results explicitly and predictably from the spatially organised initial conditions, a prepattern, and deterministic rules. For instance, a morphogen gradient programs a battery of downstream decisions that themselves dictate mechanical states in cells such as cell contractility. In contrast, self-organisation is characterized by the emergence of ordering from a purely homogenous initial state. It relies on stochastic rules, local activity, dissipation driving irreversible deformation and amplification of local activity via feedbacks that operate across scales. Thereby, the system transits to a steady-state that minimizes its free energy.

Programmed and self-organised processes differ in several other important ways that will be important to address rigorously in the future. First, the information content appears different. In programs, all steps need to be specified deterministically and a large number of parameters are tuned, as revealed in the patterning of embryos and gastrulation. In contrast, self-organised dynamics relies on very sparse information such as differential growth rates and elastic properties during buckling, differential diffusivity in Turing instabilities or differential surface tension. A simple quantitative difference in a physical parameter can produce an instability leading to an equilibrium or steady-state shape. Second, program and self-organisation exhibit different kinds of robustness, meaning resistance to internal (i.e. genetic) or external perturbations. Programs are usually hard-wired, exhibit redundancy, such that they are mostly insensitive to genetic perturbations. However, once affected, they cannot repair because of the absence of feedbacks and a strict dependency on initial conditions which may be lost as morphogenesis proceeds. In contrast, owing to their internal feedbacks, rapid dynamics, and insensitivity to initial conditions, self-organised systems can reform after complete perturbations, and constantly adapt to a changing environment. Thus, programs may be most suited to specify critical initial steps of morphogenesis where failing to properly time or position singular shape changes of the tissue may affect the entire subsequent steps of the morphogenesis, such as during embryo gastrulation or the specification of primary sulci in the developing brain cortex. However, for processes where the large number and position of deformations need not be specified precisely (e.g. feather buds, gut villi), self-organization may be more suited as the final pattern can emerge from few specified parameters stochastically. Moreover, self-organised morphogenesis is associated with repair and regeneration capacity: this is the case of the mammary gland and gut villi for instance. The development of organoids in recent years builds upon this principle.

Finally, it is important to emphasize that these two modes of information flow are idealised strategies that, as we have seen above, always coexist though one may prevail over the other during a given phase of morphogenesis. Often the result of a self-organised process produces an initial asymmetry that programs subsequent events. In embryos for instance, the initial asymmetry of the egg is usually self-organised (e.g. at fertilisation), yet the resulting polarized determinants program subsequent cellular decisions as in *C.elegans*[204]. Conversely, asymmetries that result from embryo patterning can elicit mechanical processes that subsequently propagate in a self-organised manner[42,205].

The time seems ripe to consider the new ways in which shapes not only emerge during development, but also how they evolve. Looking at information as we propose in this review provides a powerful framework for tackling this very ambitious problem.

Box1: The contrast between the 'mosaic' and the 'regulative' theories of development at the end of the XIX century

At the end of the XIX century two contrasting views of development animated the discussion between embryologists. In 1888 Wilhelm Roux published a series of experiments in which he killed with a hot needle half of the 2- or 4-cell stage frog embryos and reported that these embryos grew only half of the animal[3]. This led him to propose his 'mosaic' theory of epigenesis wherein the fate of each cell was pre-determined and fixed from the 2-cell embryo stage onwards. After few cell divisions the embryo is like a mosaic where each cell has a specific function and will give rise to different structures of the animal. In contrast with this theory, Hans Driesch in 1891 separated the two blastomeres of a 2-cell stage sea urchin embryo and found that each could give rise to a complete, although smaller embryo[13]. In line with these experiments few years later, in 1895, Thomas Morgan found that if instead of killing one of the 2 blastomeres of the 2-cell stage frog embryo (as in the case of the experiments performed by Roux), it was pipetted out, the remaining single blastomere could give rise to the entire animal, showing that the fate of cells was not fixed but rather could change according to environmental conditions. A few years later Hans Speeman showed that when a salamander embryo at the blastula stage is cut in half, if each of the halves receives part of the dorsal blastopore lip, it is able to give rise to a well-proportioned tadpole[15]. Altogether these experiments led to the 'regulative' view of development postulating that the entire early embryo constitutes a self-differentiating morphogenetic field, in which cells communicate with each other over great distances and are able to regulate each-others' choices. The 'mosaic' and the 'regulative' theories of development represent the ancestors of the current views where development is seen as deterministic or self-organized.

Box2: Length scales in mechanochemical instabilities

Patterns emerge over a range of scales, from molecular mixtures, to cellular populations in developing organisms. Irrespective of specific molecular mechanisms, Turing introduced a framework to explain how such patterns arise and symmetries are broken. In his seminal article, Turing explored how reaction and diffusion in chemical systems create heterogeneity, through local activation and long-range inhibition (left). The activator (blue) stimulates its own production and that of an inhibitor (red). If the inhibitor can diffuse faster than the activator this can locally accumulate and a stable pattern emerges from a uniform initial state by amplification of small fluctuations in concentrations of the activator and inhibitor. The length scale of the pattern depends on details of the reaction-diffusion, such as differential diffusivity. Digit number and plate ridges in the mouse are proposed to reflect chemical Turing instabilities[26,206]. Analogous instabilities arise by controlling mechanical parameters rather than molecular diffusion. For instance, the pattern of feather buds results from self-organised aggregation of mesenchymal cells migrating on an elastic substratum (middle). A local positive feedback couples an active stress associated with cell traction and an elastic stress due to ECM deformation. The elastic resistance of the matrix is akin to a long-range inhibition and tunes the spacing between cell clusters[33,34]. Actomyosin networks also produce contractile instabilities in vitro and in vivo. In the *Drosophila* trachea, rings of actin emerge from motor driven actin flow, resisted by friction within cells[35]. Flow driven advection of actin and myosin introduces a positive feedback. Frictional forces inhibit flow and reduce the length scale between actin rings. Thus mechano-chemical systems control the length scale of patterns in molecular and cellular systems.

Acknowledgements

We thank all members of the Lecuit group for stimulating discussions and useful feedback on this manuscript. The lab is supported by the ERC grant SelfControl #788308 and the Ligue contre le Cancer. C.C. is supported by the CNRS and T.L. by the Collège de France.

The authors declare no conflict of interest.

Figure legends

Figure 1: Biochemical, mechanical and geometrical nature of morphogenetic information: program versus self-organization.
a. Length- and time-scales of morphogenetic information can be defined by biochemical (in red on the left) or mechanical (in blue on the right) interactions occurring within the given geometry of the tissue (in grey). On the left the constant of effective diffusion (D) of a molecular specie (red star) from a spatially restricted production zone and its rate of degradation (*k*) define the local concentration and thus the length-scale (λ) and time-scale (τ) of the cellular and tissue level processes driving shape changes. These length- and time-scales can be quantitatively estimated by measuring D and *k* (equations in the yellow quadrant). On the right the propagation of deformation due an applied stress can define the length-scale (λ) and time-scale (τ) of morphogenetic events in a tissue. Strain propagation depends on the elastic modulus (stiffness) E, the coefficient of viscosity η and the friction coefficeint γ internal to the tissue. The length- (λ) and time-scales (τ) are defined quantitatively as in the yellow quadrant at the bottom left. Further on the right, a graphical illustration of how the viscosity of a material impacts on the time of deformation following an applied stress. A fully elastic material has a coefficient of viscosity equal to 0. Biochemical interactions and cell and tissue mechanics can regulate each other. For instance, biochemical signaling can regulate the stiffness/viscosity of the actin cortex or the activate force-generating molecular motors. Mechanics can regulate local protein concentrations by advection or elicit biochemical signaling via mechanotransdution. **b**. Idealized information flows illustrating how morphogenesis could be executed as a 'program' (middle) or emerge as self-organized (right). Biochemistry, mechanics and geometry are the key modules of morphogenesis (as illustrated in **a**). In 'programmed morphogenesis' the information is fully encapsulated in the initial patterning (i.e. biochemistry) and geometry of the tissue. This determines fully the execution of cell and tissue mechanical operations and the final outcome of morphogenesis. The strict hierarchy and the unidirectional flow of information are represented by single headed arrows. In the case of 'self-organized morphogenesis' Biochemistry, mechanics and geometry can all regulate each other as result of multiple feedbacks and thus the information emerges and is continuously updated during the morphogenetic process.

Figure 2: Polarized contractility drives tissue bending and invagination.
a. Tissue bending and deep invagination is driven by cell apical constriction followed by shortening of the lateral surfaces and widening of the cell basal sides. Patterning defines the region of bending/invagination by inducing the expression of genes (labelled in green) activating polarized contractility in cells (in orange). This in turn drives cell apical constriction and basal expansion. **b-c**. Mesoderm invagination in the *Drosophila* embryo is an example of programmed contractility-driven invagination. In the top panel: an illustration of an egg where the expression of the mesodermal genes *twist* and *snail* is indicated. **b**. A transverse section of the embryo illustrating the invagination of the mesoderm. The DV gradient of nuclear Dorsal, acting like a morphogen, defines the domain of expression of *twist* and *snail* and in turn the domain of polarized actomyosin contractility driving tissue invagination. **c**. Detailed illustration of the molecular pathway involved in the activation of polarized apical contractility. The transcription factors Twist and Snail act like master genes (green color) and drive the expression of 4 switch factors (red color): the ligand Fog, the GPCR Mist, the molecular scaffold T48. These factors activate the ubiquitous (labelled by the grey color) Rho signaling module and direct MyoII activation on the apical side of the cell. **d-e**. Posterior endoderm invagination in the *Drosophila* embryo is an example of cooperation between program and self-organization to drive morphogenesis. In the top panel: an illustration of an egg where the expression of the of the terminal patterning genes *hkb* and *tll* is indicated. **d**. A sagittal section of the embryo illustrating the invagination of the posterior endoderm. The expression *hkb* and *tll* (in green) defines the region of initial actomyosin contraction (in orange) and tissue invagination. This is followed by a wave-like propagation of actomyosin contractility beyond the region specified by patterning genes. The MyoII wave propagates by a self-organized mechanism. **e**. Detailed illustration of the self-organized propagation of MyoII contractility. MyoII contractility (in orange) in the posterior invagination and in the cell at boundary of the furrow it is anchored to the vitelline membrane through integrin-mediated adhesion (in magenta).

This leads to cell detachment and invagination and the resulting compression lifts more anterior cells inducing their adhesion to the vitelline membrane. This shifts the adhesion region more anteriorly. Then, MyoII is induced in a new cell at the boundary of the furrow re-iterating the cycle.

Figure 3: Growth-driven mechanical instabilities drive tissue folding and looping.
a. The growth of a tissue constrained between immobile boundaries drives buckling and tissue folding. **b**. The cortex the human brain is heavily folded in gyri and sulci. Brain folding has been proposed to emerge from a buckling instability where the fast growth of an external cortical layer is constrained by the slower growth of more internal layers. **c**. Differential growth of an outer and an inner layer in synthetic mini-brains obtained with compound gels with controlled stiffness gives rise to a wrinkling pattern resembling those in brain cortices. On the left a schematic of a synthetic mini-brain composed of 2 different layers of PDMS gel: an outer layer that expands by swelling which covers an inert but deformable inner layer. The stiffness of both layers can be controlled. Upon immersion in a solvent the outer layer expands by swelling inducting bending and wrinkling. On the right: representative images of the gel mini-brains before and after swelling. **d**. The looping of the small gut results from the differential growth of gut tube (blue) and of the mesentery "membrane" (orange) that connects the body to the gut tube along its entire length. **e**. Rubber model of gut looping. Sawing a stretched rubber sheet (orange) to an unstretched rubber tube along its entire length produces a looping pattern resembling those of the small intestine. **f**. The process of gut vilification in chicken embryos proceeds in steps with the emergence in a sequence of ridges, followed by zig-zags, and villi. The growth of the intestinal epithelium is sequentially constrained by the emergence of circumferential smooth muscles, followed by two layers of longitudinal muscles. Red arrows indicate the direction of growth constrained by muscle contraction (green arrows).
The images in panel **c** are adapted from ref.100, Nature Physics. Panel **e** is adapted from ref.105, Nature. Panel **f** is adapted from ref.109, Science.

Figure 4: Tissue extension by programmed polarization of cellular active stresses.
a. Illustration of convergent-extension movements driving tissue extension. **b**. Cell intercalation by cell motility drives convergent-extension in the *Xenopus* notochord and neural plate. Cells of the notochord and of the neural plate elongate, extend actin rich protrusions (in red) and intercalate by crawling onto one another in the medio-lateral direction extending the tissue in the antero-posterior direction. The cells exert traction forces on their neighbors by adhering with their actin rich protrusions and contracting their medio-laterally oriented edges. **c**. PCP signaling controls the bipolar extension of actin rich protrusion. The PCP proteins Pk and Dvl localize to mediolateral cell-cell contact and where Dvl activates Rho signaling. Antagonism between Rho and Rac signaling might explain the extension of actin rich protrusion medio-laterally. **d**. Cell intercalation by cell-cell contact remodeling drives convergence-extension in the primitive streak of chicken embryos and the germband on *Drosophila melanogaster*. Planar polarized actomyosin contractility drives cell intercalation in two steps, first the shrinkage of cell contacts in the direction of tissue convergence, followed by the extension of new contacts in the direction of tissue extension. Contractions in an apico-medial and a junctional pool of MyoII generates the forces necessary for both junction shrinkage and the subsequent extension of newly forming junctions. **e**. The planar polarized accumulation of MyoII at junctions is controlled by the global polarity of the tissue (red unidirectional arrow). PCP signaling controls this via the Celsr1 receptor in chicken embryos. In *Drosophila* embryos AP patterning controls via pair-rule genes the expression of different Toll receptors (Toll2, Toll6 and Toll8) in stripes. The striped expression of Toll receptors generates a combinatorial cell surface expression code that results in the planar polarization of MyoII at cell-cell junctions.

Figure 5: Patterned boundaries and their geometry in shape tissue flows and extension.
a-a'''. Impact of boundary configuration on tissue flow and extension. Tissue boundaries can be fixed (immobile, FB) or moving (actively or passively, MB). Both intrinsic (i.e. internal stress in green) and extrinsic (provided by actively moving boundaries, in red) stress drive tissue flow (in black). The direction of the flow is impacted by the geometry of the fixed boundaries and by the orientation of polarity cues (in magenta) guiding accumulation intrinsic stresses. In **a** internal or external stresses can elongate a tissue in a given direction. The direction of the flow depends on the orientation of internal stresses or the external stress moving the active boundary. In **a'** the direction of the flow is constrained

by the geometry of the fixed boundary. In **a''** and **a'''** the geometry of the tissue and of the fixed boundary can generate either a centripetal flow (**a''**) or a rotation (**a'''**). In **a''** tangentially oriented polarized cues orient internal stresses radially driving centripetal flow. An extrinsic centripetal stress on the moving boundary can also contribute. In **a'''** the polarity cue is oriented radially and the resulting stress is a tangential shear. This drives a rotational flow. **b-e**. Examples of the impact of moving and fixed boundaries in tissue flow and extension. **b**. In the fly wing the contraction of hinge region exerts extrinsic stresses on the wing blade orienting cell flows and the polarity of PCP proteins. The final shape of the wing depends on the pattern of attachment of the blade region to the fixed cuticle. **c**. During gastrulation in *Drosophila* embryos the invagination and movement of the posterior endoderm exerts pulling forces on the extending germbands (in blue). The egg shell provides a fixed boundary that orients the flow of the tissue. **d**. During gastrulation of *Tribolium castaneum* the serosa spreads and envelopes the contracting portion of the blastoderm which constitutes the future embryo. The direction of the flows is determined by attachment of the blastoderm to the fixed vitelline membrane and by its geometry. **e**. During gastrulation of the avian embryo the large-scale tissue flows (depicted by the gay arrows) depend on the activity of a contractile ring at the margin of the embryo. Cell divisions promote cell intercalations and sustain these flows by promoting tissue fluidization.

Figure 6: Tissue hollowing and lumen formation are controlled by mechanical and geometrical feedbacks and regulate tissue size and patterning.
a. Schematics illustrating the process of lumen formation and growth in cell doublets (on the left), as in the case of liver canaliculi, and in multicellular aggregates (middle). In both cases water flux (light blue arrows) is driven by the osmotic pressure difference $\delta\pi$ between the lumen and the surrounding cells. Active ion transport (black arrows) by pumps such as Na+/K+ ATPases fuels $\delta\pi$. The hydrostatic pressure P (blue arrows) stretches the surrounding cells and is resisted by cortical tension σ (bidirectional red arrows). The lumen grows in size up to a point of equilibrium due negative feedbacks either due to fluid leakage through cell-cell junctions (represented by leakage through short junctions on the left or through junctions weakened by cell divisions) or by reduced water flux. **b**. Illustration of the process of blastocoel formation and expansion in mouse blastocysts. The formation of a fluid filled cavity begins with the formation of hundreds of microlumens (on the left) who discharge their fluid to a single larger cavity due to pressure difference according to the Laplace law (inset). The single larger cavity forms invariantly between the trophectoderm cells (in grey) and the inner cell mass (ICM, in yellow), setting the first embryonic axis (grey arrow). Successively the blastocoel cavity grows by water influx stretching and increasing mechanical tension in TE cells and up to the point of size equilibrium due to fluid leakage during cells divisions in the TE.

Figure 7: Morphogenesis of branched structures can result from a genetic program or emerge as self-organized.
a. On the left, a picture of a developing mouse lung. In the middle, a representation of the three stereotyped modes of branching observed during development of the airways in mouse lungs. On the right, a schematic illustrating the three deterministic sequences (routines) of execution of the branching modes during the development of the branched network. Mouse lung development has been proposed to be directed by a genetically encoded "master routine" which deterministically defines which branching mode is executed at each position in the tree according to the specific routine that is being followed. **b**. Top: Cartoon representation of the branched ductal network of a mammary gland in mouse. Bottom: The branched ductal network at birth (top oval) and at the end of puberty (bottom oval). Active tips (in red) undergo stochastically one of the three behaviours illustrated on the right: they can either bifurcate giving rise to two active tips, they can proliferate elongating the ductal tube or terminate when they encounter a maturing duct. The specific dynamic features of the developing branched network (indicated by the grey text) emerge from the ensemble of stochastic behaviours of the active tips. **c**. Cartoon illustration of the development of dendritic arbour in vdpa class-I neurons in *Drosophila*. The extension of the primary branch is deterministic and follows patterned extrinsic cues (in green). Then sprouting and stabilization of the secondary and tertiary branches occurs stochastically and follows principles of self-organization. In the grey box, three local behaviours that occur stochastically and define the stabilization or retraction of secondary/tertiary branches. On the left the growth of a new tertiary branch (in orange) prevents the shrinkage of the parent branch (branch stabilization) beyond the

branch point. In the middle, new Dscam1-positive branches (orange) contact pre-existing branches (blue) and induce their retraction (induced retraction). On the right, the contact-induced inhibition (red block arrows) between two child branches orient the growth of the two parent branches (blue). Green pointed arrows indicate the direction of branch growth/shrinkage while red block arrows indicate events of contact inhibition.

References:

1 Waddington, C. H. *The Strategy of the Genes: A Discussion of Some Aspects of Theoretical Biology.* . (George Allen and Unwin, London., 1957).

2 Slack, J. M. Conrad Hal Waddington: the last Renaissance biologist? *Nat Rev Genet* **3**, 889-895, doi:10.1038/nrg933 (2002).

3 Roux, W. Contributions to the developmental mechanics of the embryo. On the artificial production of half-embryos by destruction of one of the first two blastomeres, and the later development (postgeneration) of the missing half of the body. *Foundations of Experimental Embryology*, 2-37 (1888).

4 De Robertis, E. M. Spemann's organizer and self-regulation in amphibian embryos. *Nat Rev Mol Cell Biol* **7**, 296-302, doi:10.1038/nrm1855 (2006).

5 Sulston, J. E., Schierenberg, E., White, J. G. & Thomson, J. N. The embryonic cell lineage of the nematode Caenorhabditis elegans. *Dev Biol* **100**, 64-119, doi:10.1016/0012-1606(83)90201-4 (1983).

6 Maduro, M. F. Cell fate specification in the C. elegans embryo. *Dev Dyn* **239**, 1315-1329, doi:10.1002/dvdy.22233 (2010).

7 Nishida, H. & Stach, T. Cell lineages and fate maps in tunicates: conservation and modification. *Zoolog Sci* **31**, 645-652, doi:10.2108/zs140117 (2014).

8 Garcia-Bellido, A. & Santamaria, P. Developmental analysis of the wing disc in the mutant engrailed of Drosophila melanogaster. *Genetics* **72**, 87-104 (1972).

9 Pradel, J. & White, R. A. From selectors to realizators. *Int J Dev Biol* **42**, 417-421 (1998).

10 Halder, G., Callaerts, P. & Gehring, W. J. Induction of ectopic eyes by targeted expression of the eyeless gene in Drosophila. *Science* **267**, 1788-1792, doi:10.1126/science.7892602 (1995).

11 Halder, G., Callaerts, P. & Gehring, W. J. New perspectives on eye evolution. *Curr Opin Genet Dev* **5**, 602-609, doi:10.1016/0959-437x(95)80029-8 (1995).

12 Chanut-Delalande, H., Fernandes, I., Roch, F., Payre, F. & Plaza, S. Shavenbaby couples patterning to epidermal cell shape control. *PLoS Biol* **4**, e290, doi:10.1371/journal.pbio.0040290 (2006).

13 Driesch, H. The potency of the first two cleavage cells in echinoderm development: Experimental production of double and partial formation. *Reprinted in Foundations of Experimental Embryology, BH Willier and JM Oppenheimer (eds.). Hafner, New York* (1892).

14 Morgan, T. H. Half-Embryos and Whole-Embryos from one of the first two Blastomeres of the Frog's Egg. *Anat. Anz.* **10**, 623-628 (1895).

15 Spemann, H. *Embryonic development and induction*. Vol. 10 (Taylor & Francis, 1988).

16 Browne, E. N. The production of new hydranths in Hydra by the insertion of small grafts. *Journal of Experimental Zoology* **7**, 1-23, doi:10.1002/jez.1400070102 (1909).

17 Spemann, H. & Mangold, H. Induction of embryonic primordia by implantation of organizers from a different species. *Roux's Arch Entw Mech* **100**, 599-638 (1924).

18 Gilmour, D., Rembold, M. & Leptin, M. From morphogen to morphogenesis and back. *Nature* **541**, 311-320, doi:10.1038/nature21348 (2017).

19 Hannezo, E. & Heisenberg, C. P. Mechanochemical Feedback Loops in Development and Disease. *Cell* **178**, 12-25, doi:10.1016/j.cell.2019.05.052 (2019).

20 Schweisguth, F. & Corson, F. Self-Organization in Pattern Formation. *Dev Cell* **49**, 659-677, doi:10.1016/j.devcel.2019.05.019 (2019).

21 Prusinkiewicz, P., Meinhardt, H. & Fowler, D. R. *The Algorithmic Beauty of Sea Shells*. (Springer Berlin Heidelberg, 2003).

22 Gelens, L., Anderson, G. A. & Ferrell, J. E., Jr. Spatial trigger waves: positive feedback gets you a long way. *Mol Biol Cell* **25**, 3486-3493, doi:10.1091/mbc.E14-08-1306 (2014).

23 Wartlick, O. *et al.* Dynamics of Dpp signaling and proliferation control. *Science* **331**, 1154-1159, doi:10.1126/science.1200037 (2011).

24 Rogers, K. W. & Schier, A. F. Morphogen gradients: from generation to interpretation. *Annu Rev Cell Dev Biol* **27**, 377-407, doi:10.1146/annurev-cellbio-092910-154148 (2011).

25 Sagner, A. & Briscoe, J. Morphogen interpretation: concentration, time, competence, and signaling dynamics. *Wiley Interdiscip Rev Dev Biol* **6**, doi:10.1002/wdev.271 (2017).

26 Economou, A. D. *et al.* Periodic stripe formation by a Turing mechanism operating at growth zones in the mammalian palate. *Nat Genet* **44**, 348-351, doi:10.1038/ng.1090 (2012).
27 Sheth, R. *et al.* Hox genes regulate digit patterning by controlling the wavelength of a Turing-type mechanism. *Science* **338**, 1476-1480, doi:10.1126/science.1226804 (2012).
28 Pourquie, O. The segmentation clock: converting embryonic time into spatial pattern. *Science* **301**, 328-330, doi:10.1126/science.1085887 (2003).
29 Mayer, M., Depken, M., Bois, J. S., Julicher, F. & Grill, S. W. Anisotropies in cortical tension reveal the physical basis of polarizing cortical flows. *Nature* **467**, 617-621, doi:10.1038/nature09376 (2010).
30 Clement, R., Dehapiot, B., Collinet, C., Lecuit, T. & Lenne, P. F. Viscoelastic Dissipation Stabilizes Cell Shape Changes during Tissue Morphogenesis. *Curr Biol* **27**, 3132-3142 e3134, doi:10.1016/j.cub.2017.09.005 (2017).
31 Dasbiswas, K., Hannezo, E. & Gov, N. S. Theory of Epithelial Cell Shape Transitions Induced by Mechanoactive Chemical Gradients. *Biophys J* **114**, 968-977, doi:10.1016/j.bpj.2017.12.022 (2018).
32 Dicko, M. *et al.* Geometry can provide long-range mechanical guidance for embryogenesis. *PLoS Comput Biol* **13**, e1005443, doi:10.1371/journal.pcbi.1005443 (2017).
33 Oster, G. F., Murray, J. D. & Harris, A. K. Mechanical aspects of mesenchymal morphogenesis. *J Embryol Exp Morphol* **78**, 83-125 (1983).
34 Shyer, A. E. *et al.* Emergent cellular self-organization and mechanosensation initiate follicle pattern in the avian skin. *Science* **357**, 811-815, doi:10.1126/science.aai7868 (2017).
35 Hannezo, E., Dong, B., Recho, P., Joanny, J. F. & Hayashi, S. Cortical instability drives periodic supracellular actin pattern formation in epithelial tubes. *Proc Natl Acad Sci U S A* **112**, 8620-8625, doi:10.1073/pnas.1504762112 (2015).
36 Ladoux, B., Nelson, W. J., Yan, J. & Mège, R. M. The mechanotransduction machinery at work at adherens junctions. *Integrative Biology* **7**, 1109-1119, doi:10.1039/c5ib00070j (2015).
37 Collinet, C. & Lecuit, T. Stability and dynamics of cell-cell junctions. *Prog Mol Biol Transl Sci* **116**, 25-47, doi:10.1016/B978-0-12-394311-8.00002-9 (2013).
38 Papusheva, E. & Heisenberg, C.-P. Spatial organization of adhesion: force-dependent regulation and function in tissue morphogenesis. *The EMBO Journal* **29**, 2753-2768, doi:10.1038/emboj.2010.182 (2010).
39 Schwayer, C. *et al.* Mechanosensation of Tight Junctions Depends on ZO-1 Phase Separation and Flow. *Cell* **179**, 937-952 e918, doi:10.1016/j.cell.2019.10.006 (2019).
40 Lecuit, T., Lenne, P. F. & Munro, E. Force generation, transmission, and integration during cell and tissue morphogenesis. *Annu Rev Cell Dev Biol* **27**, 157-184, doi:10.1146/annurev-cellbio-100109-104027 (2011).
41 Geiger, B., Spatz, J. P. & Bershadsky, A. D. Environmental sensing through focal adhesions. *Nat Rev Mol Cell Biol* **10**, 21-33, doi:10.1038/nrm2593 (2009).
42 Bailles, A. *et al.* Genetic induction and mechanochemical propagation of a morphogenetic wave. *Nature* **572**, 467-473, doi:10.1038/s41586-019-1492-9 (2019).
43 Kindberg, A., Hu, J. K. & Bush, J. O. Forced to communicate: Integration of mechanical and biochemical signaling in morphogenesis. *Curr Opin Cell Biol* **66**, 59-68, doi:10.1016/j.ceb.2020.05.004 (2020).
44 Munjal, A., Philippe, J. M., Munro, E. & Lecuit, T. A self-organized biomechanical network drives shape changes during tissue morphogenesis. *Nature* **524**, 351-355, doi:10.1038/nature14603 (2015).
45 Goehring, N. W. *et al.* Polarization of PAR proteins by advective triggering of a pattern-forming system. *Science* **334**, 1137-1141, doi:10.1126/science.1208619 (2011).
46 Michaux, J. B., Robin, F. B., McFadden, W. M. & Munro, E. M. Excitable RhoA dynamics drive pulsed contractions in the early C. elegans embryo. *J Cell Biol* **217**, 4230-4252, doi:10.1083/jcb.201806161 (2018).
47 Durdu, S. *et al.* Luminal signalling links cell communication to tissue architecture during organogenesis. *Nature* **515**, 120-124, doi:10.1038/nature13852 (2014).
48 Shyer, A. E., Huycke, T. R., Lee, C., Mahadevan, L. & Tabin, C. J. Bending gradients: how the intestinal stem cell gets its home. *Cell* **161**, 569-580, doi:10.1016/j.cell.2015.03.041 (2015).

49 Martin, A. C. & Goldstein, B. Apical constriction: themes and variations on a cellular mechanism driving morphogenesis. *Development* **141**, 1987-1998, doi:10.1242/dev.102228 (2014).

50 Munjal, A. & Lecuit, T. Actomyosin networks and tissue morphogenesis. *Development* **141**, 1789-1793, doi:10.1242/dev.091645 (2014).

51 Leptin, M. & Grunewald, B. Cell shape changes during gastrulation in Drosophila. *Development* **110**, 73-84 (1990).

52 Sweeton, D., Parks, S., Costa, M. & Wieschaus, E. Gastrulation in Drosophila: the formation of the ventral furrow and posterior midgut invaginations. *Development* **112**, 775-789 (1991).

53 Martin, A. C., Kaschube, M. & Wieschaus, E. F. Pulsed contractions of an actin-myosin network drive apical constriction. *Nature* **457**, 495-499, doi:10.1038/nature07522 (2009).

54 Gelbart, M. A. *et al.* Volume conservation principle involved in cell lengthening and nucleus movement during tissue morphogenesis. *Proc Natl Acad Sci U S A* **109**, 19298-19303, doi:10.1073/pnas.1205258109 (2012).

55 Krueger, D., Tardivo, P., Nguyen, C. & De Renzis, S. Downregulation of basal myosin-II is required for cell shape changes and tissue invagination. *EMBO J* **37**, doi:10.15252/embj.2018100170 (2018).

56 Gracia, M. *et al.* Mechanical impact of epithelial-mesenchymal transition on epithelial morphogenesis in Drosophila. *Nat Commun* **10**, 2951, doi:10.1038/s41467-019-10720-0 (2019).

57 Sherrard, K., Robin, F., Lemaire, P. & Munro, E. Sequential activation of apical and basolateral contractility drives ascidian endoderm invagination. *Curr Biol* **20**, 1499-1510, doi:10.1016/j.cub.2010.06.075 (2010).

58 Mason, F. M., Tworoger, M. & Martin, A. C. Apical domain polarization localizes actin-myosin activity to drive ratchet-like apical constriction. *Nat Cell Biol* **15**, 926-936, doi:10.1038/ncb2796 (2013).

59 Vasquez, C. G., Tworoger, M. & Martin, A. C. Dynamic myosin phosphorylation regulates contractile pulses and tissue integrity during epithelial morphogenesis. *J Cell Biol* **206**, 435-450, doi:10.1083/jcb.201402004 (2014).

60 Izquierdo, E., Quinkler, T. & De Renzis, S. Guided morphogenesis through optogenetic activation of Rho signalling during early Drosophila embryogenesis. *Nat Commun* **9**, 2366, doi:10.1038/s41467-018-04754-z (2018).

61 Reeves, G. T. & Stathopoulos, A. Graded dorsal and differential gene regulation in the Drosophila embryo. *Cold Spring Harb Perspect Biol* **1**, a000836, doi:10.1101/cshperspect.a000836 (2009).

62 Manning, A. J., Peters, K. A., Peifer, M. & Rogers, S. L. Regulation of epithelial morphogenesis by the G protein-coupled receptor mist and its ligand fog. *Sci Signal* **6**, ra98, doi:10.1126/scisignal.2004427 (2013).

63 Costa, M., Wilson, E. T. & Wieschaus, E. A putative cell signal encoded by the folded gastrulation gene coordinates cell shape changes during Drosophila gastrulation. *Cell* **76**, 1075-1089 (1994).

64 Kolsch, V., Seher, T., Fernandez-Ballester, G. J., Serrano, L. & Leptin, M. Control of Drosophila gastrulation by apical localization of adherens junctions and RhoGEF2. *Science* **315**, 384-386, doi:10.1126/science.1134833 (2007).

65 Lee, J. Y. *et al.* Wnt/Frizzled signaling controls C. elegans gastrulation by activating actomyosin contractility. *Curr Biol* **16**, 1986-1997, doi:10.1016/j.cub.2006.08.090 (2006).

66 Roh-Johnson, M. *et al.* Triggering a cell shape change by exploiting preexisting actomyosin contractions. *Science* **335**, 1232-1235, doi:10.1126/science.1217869 (2012).

67 Marston, D. J. *et al.* MRCK-1 Drives Apical Constriction in C. elegans by Linking Developmental Patterning to Force Generation. *Curr Biol* **26**, 2079-2089, doi:10.1016/j.cub.2016.06.010 (2016).

68 Nishimura, T. & Takeichi, M. Shroom3-mediated recruitment of Rho kinases to the apical cell junctions regulates epithelial and neuroepithelial planar remodeling. *Development* **135**, 1493-1502, doi:10.1242/dev.019646 (2008).

69 Haigo, S. L., Hildebrand, J. D., Harland, R. M. & Wallingford, J. B. Shroom induces apical constriction and is required for hingepoint formation during neural tube closure. *Curr Biol* **13**, 2125-2137, doi:10.1016/j.cub.2003.11.054 (2003).
70 Chung, M. I., Nascone-Yoder, N. M., Grover, S. A., Drysdale, T. A. & Wallingford, J. B. Direct activation of Shroom3 transcription by Pitx proteins drives epithelial morphogenesis in the developing gut. *Development* **137**, 1339-1349, doi:10.1242/dev.044610 (2010).
71 Plageman, T. F., Jr. *et al.* Pax6-dependent Shroom3 expression regulates apical constriction during lens placode invagination. *Development* **137**, 405-415, doi:10.1242/dev.045369 (2010).
72 Plageman, T. F., Jr. *et al.* A Trio-RhoA-Shroom3 pathway is required for apical constriction and epithelial invagination. *Development* **138**, 5177-5188, doi:10.1242/dev.067868 (2011).
73 Ernst, S. *et al.* Shroom3 is required downstream of FGF signalling to mediate proneuromast assembly in zebrafish. *Development* **139**, 4571-4581, doi:10.1242/dev.083253 (2012).
74 Hildebrand, J. D. Shroom regulates epithelial cell shape via the apical positioning of an actomyosin network. *J Cell Sci* **118**, 5191-5203, doi:10.1242/jcs.02626 (2005).
75 Lang, R. A., Herman, K., Reynolds, A. B., Hildebrand, J. D. & Plageman, T. F., Jr. p120-catenin-dependent junctional recruitment of Shroom3 is required for apical constriction during lens pit morphogenesis. *Development* **141**, 3177-3187, doi:10.1242/dev.107433 (2014).
76 Rauzi, M., Lenne, P. F. & Lecuit, T. Planar polarized actomyosin contractile flows control epithelial junction remodelling. *Nature* **468**, 1110-1114, doi:10.1038/nature09566 (2010).
77 Solon, J., Kaya-Copur, A., Colombelli, J. & Brunner, D. Pulsed forces timed by a ratchet-like mechanism drive directed tissue movement during dorsal closure. *Cell* **137**, 1331-1342, doi:10.1016/j.cell.2009.03.050 (2009).
78 Munro, E., Nance, J. & Priess, J. R. Cortical flows powered by asymmetrical contraction transport PAR proteins to establish and maintain anterior-posterior polarity in the early C. elegans embryo. *Dev Cell* **7**, 413-424, doi:10.1016/j.devcel.2004.08.001 (2004).
79 Kim, H. Y. & Davidson, L. A. Punctuated actin contractions during convergent extension and their permissive regulation by the non-canonical Wnt-signaling pathway. *J Cell Sci* **124**, 635-646, doi:10.1242/jcs.067579 (2011).
80 Maitre, J. L., Niwayama, R., Turlier, H., Nedelec, F. & Hiiragi, T. Pulsatile cell-autonomous contractility drives compaction in the mouse embryo. *Nat Cell Biol* **17**, 849-855, doi:10.1038/ncb3185 (2015).
81 Xie, S. & Martin, A. C. Intracellular signalling and intercellular coupling coordinate heterogeneous contractile events to facilitate tissue folding. *Nat Commun* **6**, 7161, doi:10.1038/ncomms8161 (2015).
82 Yevick, H. G., Miller, P. W., Dunkel, J. & Martin, A. C. Structural Redundancy in Supracellular Actomyosin Networks Enables Robust Tissue Folding. *Dev Cell* **50**, 586-598 e583, doi:10.1016/j.devcel.2019.06.015 (2019).
83 Bhide, S. *et al.* Mechanical competition alters the cellular interpretation of an endogenous genetic programme. *bioRxiv*, 2020.2010.2015.333963, doi:10.1101/2020.10.15.333963 (2020).
84 Odell, G. M., Oster, G., Alberch, P. & Burnside, B. The mechanical basis of morphogenesis. I. Epithelial folding and invagination. *Dev Biol* **85**, 446-462 (1981).
85 Llinares-Benadero, C. & Borrell, V. Deconstructing cortical folding: genetic, cellular and mechanical determinants. *Nat Rev Neurosci* **20**, 161-176, doi:10.1038/s41583-018-0112-2 (2019).
86 Garcia, K. E., Kroenke, C. D. & Bayly, P. V. Mechanics of cortical folding: stress, growth and stability. *Philos Trans R Soc Lond B Biol Sci* **373**, doi:10.1098/rstb.2017.0321 (2018).
87 Huycke, T. R. & Tabin, C. J. Chick midgut morphogenesis. *Int J Dev Biol* **62**, 109-119, doi:10.1387/ijdb.170325ct (2018).
88 Walton, K. D., Mishkind, D., Riddle, M. R., Tabin, C. J. & Gumucio, D. L. Blueprint for an intestinal villus: Species-specific assembly required. *Wiley Interdiscip Rev Dev Biol* **7**, e317, doi:10.1002/wdev.317 (2018).
89 Vasung, L. *et al.* Quantitative and Qualitative Analysis of Transient Fetal Compartments during Prenatal Human Brain Development. *Front Neuroanat* **10**, 11, doi:10.3389/fnana.2016.00011 (2016).

90 Neal, J. *et al.* Insights into the gyrification of developing ferret brain by magnetic resonance imaging. *J Anat* **210**, 66-77, doi:10.1111/j.1469-7580.2006.00674.x (2007).
91 Lohmann, G., von Cramon, D. Y. & Colchester, A. C. Deep sulcal landmarks provide an organizing framework for human cortical folding. *Cereb Cortex* **18**, 1415-1420, doi:10.1093/cercor/bhm174 (2008).
92 Ono, M., Kubik, S. & Abernathey, C. D. *Atlas of the Cerebral Sulci*. (G. Thieme Verlag, 1990).
93 Mota, B. & Herculano-Houzel, S. BRAIN STRUCTURE. Cortical folding scales universally with surface area and thickness, not number of neurons. *Science* **349**, 74-77, doi:10.1126/science.aaa9101 (2015).
94 Van Essen, D. C. A tension-based theory of morphogenesis and compact wiring in the central nervous system. *Nature* **385**, 313-318, doi:10.1038/385313a0 (1997).
95 Lefevre, J. & Mangin, J. F. A reaction-diffusion model of human brain development. *PLoS Comput Biol* **6**, e1000749, doi:10.1371/journal.pcbi.1000749 (2010).
96 Richman, D. P., Stewart, R. M., Hutchinson, J. W. & Caviness, V. S., Jr. Mechanical model of brain convolutional development. *Science* **189**, 18-21, doi:10.1126/science.1135626 (1975).
97 Hannezo, E., Prost, J. & Joanny, J. F. Instabilities of monolayered epithelia: shape and structure of villi and crypts. *Phys Rev Lett* **107**, 078104, doi:10.1103/PhysRevLett.107.078104 (2011).
98 Ben Amar, M. & Jia, F. Anisotropic growth shapes intestinal tissues during embryogenesis. *Proc Natl Acad Sci U S A* **110**, 10525-10530, doi:10.1073/pnas.1217391110 (2013).
99 Mahadevan, L. & Rica, S. Self-organized origami. *Science* **307**, 1740, doi:10.1126/science.1105169 (2005).
100 Xu, G. *et al.* Axons pull on the brain, but tension does not drive cortical folding. *J Biomech Eng* **132**, 071013, doi:10.1115/1.4001683 (2010).
101 Tallinen, T., Chung, J. Y., Biggins, J. S. & Mahadevan, L. Gyrification from constrained cortical expansion. *Proc Natl Acad Sci U S A* **111**, 12667-12672, doi:10.1073/pnas.1406015111 (2014).
102 Tallinen, T. *et al.* On the growth and form of cortical convolutions. *Nat Phys* **12**, 588-593, doi:10.1038/Nphys3632 (2016).
103 Kriegstein, A., Noctor, S. & Martinez-Cerdeno, V. Patterns of neural stem and progenitor cell division may underlie evolutionary cortical expansion. *Nat Rev Neurosci* **7**, 883-890, doi:10.1038/nrn2008 (2006).
104 Smart, I. H., Dehay, C., Giroud, P., Berland, M. & Kennedy, H. Unique morphological features of the proliferative zones and postmitotic compartments of the neural epithelium giving rise to striate and extrastriate cortex in the monkey. *Cereb Cortex* **12**, 37-53, doi:10.1093/cercor/12.1.37 (2002).
105 Reillo, I., de Juan Romero, C., Garcia-Cabezas, M. A. & Borrell, V. A role for intermediate radial glia in the tangential expansion of the mammalian cerebral cortex. *Cereb Cortex* **21**, 1674-1694, doi:10.1093/cercor/bhq238 (2011).
106 de Juan Romero, C., Bruder, C., Tomasello, U., Sanz-Anquela, J. M. & Borrell, V. Discrete domains of gene expression in germinal layers distinguish the development of gyrencephaly. *EMBO J* **34**, 1859-1874, doi:10.15252/embj.201591176 (2015).
107 Savin, T. *et al.* On the growth and form of the gut. *Nature* **476**, 57-62, doi:10.1038/nature10277 (2011).
108 Lyons, K. M., Pelton, R. W. & Hogan, B. L. Organogenesis and pattern formation in the mouse: RNA distribution patterns suggest a role for bone morphogenetic protein-2A (BMP-2A). *Development* **109**, 833-844 (1990).
109 Nerurkar, N. L., Mahadevan, L. & Tabin, C. J. BMP signaling controls buckling forces to modulate looping morphogenesis of the gut. *Proc Natl Acad Sci U S A* **114**, 2277-2282, doi:10.1073/pnas.1700307114 (2017).
110 Coulombre, A. J. & Coulombre, J. L. Intestinal development. I. Morphogenesis of the villi and musculature. *J Embryol Exp Morphol* **6**, 403-411 (1958).
111 Shyer, A. E. *et al.* Villification: How the Gut Gets Its Villi. *Science* **342**, 212-218, doi:10.1126/science.1238842 (2013).
112 Grey, R. D. Morphogenesis of intestinal villi. I. Scanning electron microscopy of the duodenal epithelium of the developing chick embryo. *J Morphol* **137**, 193-213, doi:10.1002/jmor.1051370206 (1972).

113 Burgess, D. R. Morphogenesis of intestinal villi. II. Mechanism of formation of previllous ridges. *J Embryol Exp Morphol* **34**, 723-740 (1975).
114 Walton, K. D., Freddo, A. M., Wang, S. & Gumucio, D. L. Generation of intestinal surface: an absorbing tale. *Development* **143**, 2261-2272, doi:10.1242/dev.135400 (2016).
115 Walton, K. D. *et al.* Villification in the mouse: Bmp signals control intestinal villus patterning. *Development* **143**, 427-436, doi:10.1242/dev.130112 (2016).
116 Harris, A. K., Stopak, D. & Warner, P. Generation of spatially periodic patterns by a mechanical instability: a mechanical alternative to the Turing model. *J Embryol Exp Morphol* **80**, 1-20 (1984).
117 Devenport, D. Tissue morphodynamics: Translating planar polarity cues into polarized cell behaviors. *Semin Cell Dev Biol* **55**, 99-110, doi:10.1016/j.semcdb.2016.03.012 (2016).
118 Shindo, A. Models of convergent extension during morphogenesis. *Wiley Interdiscip Rev Dev Biol* **7**, doi:10.1002/wdev.293 (2018).
119 Huebner, R. J. & Wallingford, J. B. Coming to Consensus: A Unifying Model Emerges for Convergent Extension. *Dev Cell* **46**, 389-396, doi:10.1016/j.devcel.2018.08.003 (2018).
120 Keller, R. & Tibbetts, P. Mediolateral cell intercalation in the dorsal, axial mesoderm of Xenopus laevis. *Dev Biol* **131**, 539-549, doi:10.1016/s0012-1606(89)80024-7 (1989).
121 Wilson, P. & Keller, R. Cell rearrangement during gastrulation of Xenopus: direct observation of cultured explants. *Development* **112**, 289-300 (1991).
122 Shih, J. & Keller, R. Patterns of cell motility in the organizer and dorsal mesoderm of Xenopus laevis. *Development* **116**, 915-930 (1992).
123 Shih, J. & Keller, R. Cell motility driving mediolateral intercalation in explants of Xenopus laevis. *Development* **116**, 901-914 (1992).
124 Davidson, L. A., Marsden, M., Keller, R. & Desimone, D. W. Integrin alpha5beta1 and fibronectin regulate polarized cell protrusions required for Xenopus convergence and extension. *Curr Biol* **16**, 833-844, doi:10.1016/j.cub.2006.03.038 (2006).
125 Skoglund, P., Rolo, A., Chen, X., Gumbiner, B. M. & Keller, R. Convergence and extension at gastrulation require a myosin IIB-dependent cortical actin network. *Development* **135**, 2435-2444, doi:10.1242/dev.014704 (2008).
126 Munro, E. M. & Odell, G. M. Polarized basolateral cell motility underlies invagination and convergent extension of the ascidian notochord. *Development* **129**, 13-24 (2002).
127 Williams-Masson, E. M., Heid, P. J., Lavin, C. A. & Hardin, J. The cellular mechanism of epithelial rearrangement during morphogenesis of the Caenorhabditis elegans dorsal hypodermis. *Dev Biol* **204**, 263-276, doi:10.1006/dbio.1998.9048 (1998).
128 Walck-Shannon, E., Reiner, D. & Hardin, J. Polarized Rac-dependent protrusions drive epithelial intercalation in the embryonic epidermis of C. elegans. *Development* **142**, 3549-3560, doi:10.1242/dev.127597 (2015).
129 Sun, Z. *et al.* Basolateral protrusion and apical contraction cooperatively drive Drosophila germband extension. *Nat Cell Biol* **19**, 375-383, doi:10.1038/ncb3497 (2017).
130 Williams, M., Yen, W., Lu, X. & Sutherland, A. Distinct apical and basolateral mechanisms drive planar cell polarity-dependent convergent extension of the mouse neural plate. *Dev Cell* **29**, 34-46, doi:10.1016/j.devcel.2014.02.007 (2014).
131 Irvine, K. D. & Wieschaus, E. Cell intercalation during Drosophila germband extension and its regulation by pair-rule segmentation genes. *Development* **120**, 827-841 (1994).
132 Bertet, C., Sulak, L. & Lecuit, T. Myosin-dependent junction remodelling controls planar cell intercalation and axis elongation. *Nature* **429**, 667-671, doi:10.1038/nature02590 (2004).
133 Blankenship, J. T., Backovic, S. T., Sanny, J. S., Weitz, O. & Zallen, J. A. Multicellular rosette formation links planar cell polarity to tissue morphogenesis. *Dev Cell* **11**, 459-470, doi:10.1016/j.devcel.2006.09.007 (2006).
134 Fernandez-Gonzalez, R. & Zallen, J. A. Oscillatory behaviors and hierarchical assembly of contractile structures in intercalating cells. *Phys Biol* **8**, 045005, doi:10.1088/1478-3975/8/4/045005 (2011).
135 Collinet, C., Rauzi, M., Lenne, P. F. & Lecuit, T. Local and tissue-scale forces drive oriented junction growth during tissue extension. *Nat Cell Biol* **17**, 1247-1258, doi:10.1038/ncb3226 (2015).

136 Yu, J. C. & Fernandez-Gonzalez, R. Local mechanical forces promote polarized junctional assembly and axis elongation in Drosophila. *Elife* **5**, doi:10.7554/eLife.10757 (2016).
137 Rauzi, M., Verant, P., Lecuit, T. & Lenne, P. F. Nature and anisotropy of cortical forces orienting Drosophila tissue morphogenesis. *Nat Cell Biol* **10**, 1401-1410, doi:10.1038/ncb1798 (2008).
138 Fernandez-Gonzalez, R., Simoes Sde, M., Roper, J. C., Eaton, S. & Zallen, J. A. Myosin II dynamics are regulated by tension in intercalating cells. *Dev Cell* **17**, 736-743, doi:10.1016/j.devcel.2009.09.003 (2009).
139 Bambardekar, K., Clement, R., Blanc, O., Chardes, C. & Lenne, P. F. Direct laser manipulation reveals the mechanics of cell contacts in vivo. *Proc Natl Acad Sci U S A* **112**, 1416-1421, doi:10.1073/pnas.1418732112 (2015).
140 Kale, G. R. *et al.* Distinct contributions of tensile and shear stress on E-cadherin levels during morphogenesis. *Nat Commun* **9**, 5021, doi:10.1038/s41467-018-07448-8 (2018).
141 Rozbicki, E. *et al.* Myosin-II-mediated cell shape changes and cell intercalation contribute to primitive streak formation. *Nat Cell Biol* **17**, 397-408, doi:10.1038/ncb3138 (2015).
142 Nishimura, T., Honda, H. & Takeichi, M. Planar cell polarity links axes of spatial dynamics in neural-tube closure. *Cell* **149**, 1084-1097, doi:10.1016/j.cell.2012.04.021 (2012).
143 Shindo, A. & Wallingford, J. B. PCP and septins compartmentalize cortical actomyosin to direct collective cell movement. *Science* **343**, 649-652, doi:10.1126/science.1243126 (2014).
144 Shindo, A., Inoue, Y., Kinoshita, M. & Wallingford, J. B. PCP-dependent transcellular regulation of actomyosin oscillation facilitates convergent extension of vertebrate tissue. *Dev Biol* **446**, 159-167, doi:10.1016/j.ydbio.2018.12.017 (2019).
145 Zallen, J. A. & Wieschaus, E. Patterned gene expression directs bipolar planar polarity in Drosophila. *Dev Cell* **6**, 343-355, doi:10.1016/s1534-5807(04)00060-7 (2004).
146 Pare, A. C. *et al.* A positional Toll receptor code directs convergent extension in Drosophila. *Nature* **515**, 523-527, doi:10.1038/nature13953 (2014).
147 Lavalou, J. *et al.* Formation of mechanical interfaces by self-organized Toll-8/Cirl GPCR asymmetry. *bioRxiv*, 2020.2003.2016.993758, doi:10.1101/2020.03.16.993758 (2020).
148 Wallingford, J. B. Planar cell polarity and the developmental control of cell behavior in vertebrate embryos. *Annu Rev Cell Dev Biol* **28**, 627-653, doi:10.1146/annurev-cellbio-092910-154208 (2012).
149 Yang, Y. & Mlodzik, M. Wnt-Frizzled/planar cell polarity signaling: cellular orientation by facing the wind (Wnt). *Annu Rev Cell Dev Biol* **31**, 623-646, doi:10.1146/annurev-cellbio-100814-125315 (2015).
150 Butler, M. T. & Wallingford, J. B. Planar cell polarity in development and disease. *Nat Rev Mol Cell Biol* **18**, 375-388, doi:10.1038/nrm.2017.11 (2017).
151 Strutt, D. I., Weber, U. & Mlodzik, M. The role of RhoA in tissue polarity and Frizzled signalling. *Nature* **387**, 292-295, doi:10.1038/387292a0 (1997).
152 Winter, C. G. *et al.* Drosophila Rho-associated kinase (Drok) links Frizzled-mediated planar cell polarity signaling to the actin cytoskeleton. *Cell* **105**, 81-91, doi:10.1016/s0092-8674(01)00298-7 (2001).
153 Andreeva, A. *et al.* PTK7-Src signaling at epithelial cell contacts mediates spatial organization of actomyosin and planar cell polarity. *Dev Cell* **29**, 20-33, doi:10.1016/j.devcel.2014.02.008 (2014).
154 Habas, R., Dawid, I. B. & He, X. Coactivation of Rac and Rho by Wnt/Frizzled signaling is required for vertebrate gastrulation. *Genes Dev* **17**, 295-309, doi:10.1101/gad.1022203 (2003).
155 Heisenberg, C. P. *et al.* Silberblick/Wnt11 mediates convergent extension movements during zebrafish gastrulation. *Nature* **405**, 76-81, doi:10.1038/35011068 (2000).
156 Wallingford, J. B. *et al.* Dishevelled controls cell polarity during Xenopus gastrulation. *Nature* **405**, 81-85, doi:10.1038/35011077 (2000).
157 Keys, D. N., Levine, M., Harland, R. M. & Wallingford, J. B. Control of intercalation is cell-autonomous in the notochord of Ciona intestinalis. *Dev Biol* **246**, 329-340, doi:10.1006/dbio.2002.0656 (2002).
158 Butler, M. T. & Wallingford, J. B. Spatial and temporal analysis of PCP protein dynamics during neural tube closure. *Elife* **7**, doi:10.7554/eLife.36456 (2018).

159 Habas, R., Kato, Y. & He, X. Wnt/Frizzled activation of Rho regulates vertebrate gastrulation and requires a novel Formin homology protein Daam1. *Cell* **107**, 843-854, doi:10.1016/s0092-8674(01)00614-6 (2001).
160 Kim, S. K. *et al.* Planar cell polarity acts through septins to control collective cell movement and ciliogenesis. *Science* **329**, 1337-1340, doi:10.1126/science.1191184 (2010).
161 Levayer, R. & Lecuit, T. Oscillation and polarity of E-cadherin asymmetries control actomyosin flow patterns during morphogenesis. *Dev Cell* **26**, 162-175, doi:10.1016/j.devcel.2013.06.020 (2013).
162 Lye, C. M. *et al.* Mechanical Coupling between Endoderm Invagination and Axis Extension in Drosophila. *PLoS Biol* **13**, e1002292, doi:10.1371/journal.pbio.1002292 (2015).
163 Saadaoui, M., Rocancourt, D., Roussel, J., Corson, F. & Gros, J. A tensile ring drives tissue flows to shape the gastrulating amniote embryo. *Science* **367**, 453-458, doi:10.1126/science.aaw1965 (2020).
164 Aigouy, B. *et al.* Cell flow reorients the axis of planar polarity in the wing epithelium of Drosophila. *Cell* **142**, 773-786, doi:10.1016/j.cell.2010.07.042 (2010).
165 Etournay, R. *et al.* Interplay of cell dynamics and epithelial tension during morphogenesis of the Drosophila pupal wing. *Elife* **4**, e07090, doi:10.7554/eLife.07090 (2015).
166 Ray, R. P. *et al.* Patterned Anchorage to the Apical Extracellular Matrix Defines Tissue Shape in the Developing Appendages of Drosophila. *Dev Cell* **34**, 310-322, doi:10.1016/j.devcel.2015.06.019 (2015).
167 Munster, S. *et al.* Attachment of the blastoderm to the vitelline envelope affects gastrulation of insects. *Nature* **568**, 395-399, doi:10.1038/s41586-019-1044-3 (2019).
168 Sato, K. *et al.* Left-right asymmetric cell intercalation drives directional collective cell movement in epithelial morphogenesis. *Nat Commun* **6**, 10074, doi:10.1038/ncomms10074 (2015).
169 Coulombre, A. J. The role of intraocular pressure in the development of the chick eye. II. Control of corneal size. *AMA Arch Ophthalmol* **57**, 250-253, doi:10.1001/archopht.1957.00930050260015 (1957).
170 Desmond, M. E. & Jacobson, A. G. Embryonic brain enlargement requires cerebrospinal fluid pressure. *Dev Biol* **57**, 188-198, doi:10.1016/0012-1606(77)90364-5 (1977).
171 Abbas, L. & Whitfield, T. T. Nkcc1 (Slc12a2) is required for the regulation of endolymph volume in the otic vesicle and swim bladder volume in the zebrafish larva. *Development* **136**, 2837-2848, doi:10.1242/dev.034215 (2009).
172 Navis, A., Marjoram, L. & Bagnat, M. Cftr controls lumen expansion and function of Kupffer's vesicle in zebrafish. *Development* **140**, 1703-1712, doi:10.1242/dev.091819 (2013).
173 Ruiz-Herrero, T., Alessandri, K., Gurchenkov, B. V., Nassoy, P. & Mahadevan, L. Organ size control via hydraulically gated oscillations. *Development* **144**, 4422-4427, doi:10.1242/dev.153056 (2017).
174 Dasgupta, S., Gupta, K., Zhang, Y., Viasnoff, V. & Prost, J. Physics of lumen growth. *Proc Natl Acad Sci U S A* **115**, E4751-E4757, doi:10.1073/pnas.1722154115 (2018).
175 Chan, C. J. *et al.* Hydraulic control of mammalian embryo size and cell fate. *Nature* **571**, 112-116, doi:10.1038/s41586-019-1309-x (2019).
176 Bryant, D. M. & Mostov, K. E. From cells to organs: building polarized tissue. *Nat Rev Mol Cell Biol* **9**, 887-901, doi:10.1038/nrm2523 (2008).
177 Sigurbjornsdottir, S., Mathew, R. & Leptin, M. Molecular mechanisms of de novo lumen formation. *Nat Rev Mol Cell Biol* **15**, 665-676, doi:10.1038/nrm3871 (2014).
178 Sperber, I. Secretion of organic anions in the formation of urine and bile. *Pharmacol Rev* **11**, 109-134 (1959).
179 Boyer, J. L. Bile formation and secretion. *Compr Physiol* **3**, 1035-1078, doi:10.1002/cphy.c120027 (2013).
180 Navis, A. & Bagnat, M. Developing pressures: fluid forces driving morphogenesis. *Curr Opin Genet Dev* **32**, 24-30, doi:10.1016/j.gde.2015.01.010 (2015).
181 Navis, A. & Nelson, C. M. Pulling together: Tissue-generated forces that drive lumen morphogenesis. *Semin Cell Dev Biol* **55**, 139-147, doi:10.1016/j.semcdb.2016.01.002 (2016).

182 Mosaliganti, K. R. *et al.* Size control of the inner ear via hydraulic feedback. *Elife* **8**, doi:10.7554/eLife.39596 (2019).
183 Takaoka, K. & Hamada, H. Cell fate decisions and axis determination in the early mouse embryo. *Development* **139**, 3-14, doi:10.1242/dev.060095 (2012).
184 Dumortier, J. G. *et al.* Hydraulic fracturing and active coarsening position the lumen of the mouse blastocyst. *Science* **365**, 465-468, doi:10.1126/science.aaw7709 (2019).
185 Maitre, J. L. *et al.* Asymmetric division of contractile domains couples cell positioning and fate specification. *Nature* **536**, 344-348, doi:10.1038/nature18958 (2016).
186 Samarage, C. R. *et al.* Cortical Tension Allocates the First Inner Cells of the Mammalian Embryo. *Dev Cell* **34**, 435-447, doi:10.1016/j.devcel.2015.07.004 (2015).
187 Plusa, B. *et al.* Downregulation of Par3 and aPKC function directs cells towards the ICM in the preimplantation mouse embryo. *J Cell Sci* **118**, 505-515, doi:10.1242/jcs.01666 (2005).
188 Nishioka, N. *et al.* The Hippo signaling pathway components Lats and Yap pattern Tead4 activity to distinguish mouse trophectoderm from inner cell mass. *Dev Cell* **16**, 398-410, doi:10.1016/j.devcel.2009.02.003 (2009).
189 Korotkevich, E. *et al.* The Apical Domain Is Required and Sufficient for the First Lineage Segregation in the Mouse Embryo. *Dev Cell* **40**, 235-247 e237, doi:10.1016/j.devcel.2017.01.006 (2017).
190 Ryan, A. Q., Chan, C. J., Graner, F. & Hiiragi, T. Lumen Expansion Facilitates Epiblast-Primitive Endoderm Fate Specification during Mouse Blastocyst Formation. *Dev Cell* **51**, 684-697 e684, doi:10.1016/j.devcel.2019.10.011 (2019).
191 Metzger, R. J. & Krasnow, M. A. Genetic control of branching morphogenesis. *Science* **284**, 1635-1639, doi:10.1126/science.284.5420.1635 (1999).
192 Affolter, M., Zeller, R. & Caussinus, E. Tissue remodelling through branching morphogenesis. *Nat Rev Mol Cell Biol* **10**, 831-842, doi:10.1038/nrm2797 (2009).
193 Ochoa-Espinosa, A. & Affolter, M. Branching morphogenesis: from cells to organs and back. *Cold Spring Harb Perspect Biol* **4**, doi:10.1101/cshperspect.a008243 (2012).
194 Affolter, M. & Caussinus, E. Tracheal branching morphogenesis in Drosophila: new insights into cell behaviour and organ architecture. *Development* **135**, 2055-2064, doi:10.1242/dev.014498 (2008).
195 Sutherland, D., Samakovlis, C. & Krasnow, M. A. branchless encodes a Drosophila FGF homolog that controls tracheal cell migration and the pattern of branching. *Cell* **87**, 1091-1101, doi:10.1016/s0092-8674(00)81803-6 (1996).
196 Metzger, R. J., Klein, O. D., Martin, G. R. & Krasnow, M. A. The branching programme of mouse lung development. *Nature* **453**, 745-750, doi:10.1038/nature07005 (2008).
197 Hannezo, E. *et al.* A Unifying Theory of Branching Morphogenesis. *Cell* **171**, 242-255 e227, doi:10.1016/j.cell.2017.08.026 (2017).
198 Halevi, S. *et al.* The C. elegans ric-3 gene is required for maturation of nicotinic acetylcholine receptors. *EMBO J* **21**, 1012-1020, doi:10.1093/emboj/21.5.1012 (2002).
199 Tsalik, E. L. *et al.* LIM homeobox gene-dependent expression of biogenic amine receptors in restricted regions of the C. elegans nervous system. *Dev Biol* **263**, 81-102, doi:10.1016/s0012-1606(03)00447-0 (2003).
200 Dong, X., Liu, O. W., Howell, A. S. & Shen, K. An extracellular adhesion molecule complex patterns dendritic branching and morphogenesis. *Cell* **155**, 296-307, doi:10.1016/j.cell.2013.08.059 (2013).
201 Salzberg, Y. *et al.* Skin-derived cues control arborization of sensory dendrites in Caenorhabditis elegans. *Cell* **155**, 308-320, doi:10.1016/j.cell.2013.08.058 (2013).
202 Zou, W. *et al.* A multi-protein receptor-ligand complex underlies combinatorial dendrite guidance choices in C. elegans. *Elife* **5**, doi:10.7554/eLife.18345 (2016).
203 Palavalli, A., Tizón-Escamilla, N., Rupprecht, J.-F. & Lecuit, T. Deterministic and stochastic rules of branching govern dendritic morphogenesis of sensory neurons. *bioRxiv*, 2020.2007.2011.198309, doi:10.1101/2020.07.11.198309 (2020).
204 Munro, E. & Bowerman, B. Cellular symmetry breaking during Caenorhabditis elegans development. *Cold Spring Harb Perspect Biol* **1**, a003400, doi:10.1101/cshperspect.a003400 (2009).

205 Hashimoto, H., Robin, F. B., Sherrard, K. M. & Munro, E. M. Sequential contraction and exchange of apical junctions drives zippering and neural tube closure in a simple chordate. *Dev Cell* **32**, 241-255, doi:10.1016/j.devcel.2014.12.017 (2015).

206 Green, J. B. & Sharpe, J. Positional information and reaction-diffusion: two big ideas in developmental biology combine. *Development* **142**, 1203-1211, doi:10.1242/dev.114991 (2015).

Glossary terms

Denticles: small cuticular bristles on the ventral side of Drosophila larvae which are used for locomotion.

Reaction-diffusion systems: Mathematical models describing the change in space and time of the concentration of one or more chemical substances. They typically consider local chemical reactions producing/consuming chemical species and their diffusion.

Turing instability: A reaction-diffusion system in which the homogeneous equilibrium of mixed chemical substances is unstable due to random fluctuations and differential diffusion. This gives rise to stationary wave patterns.

Morphogenetic fields: A group of cells responding to discrete, localized biochemical signals leading to the development of specific morphological structures or organs.

Mechanical stress: a physical quantity that expresses the mechanical forces that neighbouring particles of a continuous material exert on each other.

Strain: deformation of an object upon application of a mechanical stress.

Viscous response: Deformation of a viscous element, which resists shear flow and strain linearly with time when a stress is applied.

Boundary conditions: Constraints defining the limits of a system. In the case of morphogenesis these are typically the physical boundary of a tissue or an embryo.

Zebrafish lateral line: a sensory system comprised of clusters of mechanosensory epithelial cells (neuromasts) arranged as rosettes with their apical surface facing a shared lumen. The lateral line is initially established by a migratory group of cells, called a primordium, that deposits neuromasts at stereotyped locations along the surface of the fish.

Mena and VASP: members of the VASP (VAsodilator-Stimulated Phosphoprotein) family of proteins regulating the dynamics of the cortical actin cytoskeleton as downstream effectors of the Rho-family small G-proteins Rac and Cdc42.

Shroom family proteins: family of proteins characterized by a specific arrangement of an N-terminal PDZ domain, a central ASD1 (Apx/Shrm Domain 1) motif and a C-terminal ASD2 motif. ASD1 is required for targeting actin, while ASD2 is capable of eliciting an actomyosin constriction event.

Convergent–extension: the process by which a tissue changes shape by narrowing (converging) in one direction and extending along a perpendicular axis.

Traction forces: forces used to generate motion between a body and a tangential surface, through the use of friction or adhesion. Contractile systems anchored to a rigid body can generate traction forces to move cells or cellular objects.

Notochord: a small flexible rod made from cells from the mesoderm and oriented head to tail in embryos of organisms of the phylum *chordata*. Since it is composed of stiffer tissue, it allows for skeletal support of the embryo during development.

Germband: blastoderm tissue corresponding to the ventrolateral region of the embryo in *Drosophila melanogaster* and other insects.

Primitive streak: transient structure that forms in the blastula during the early stages of avian, reptilian and mammalian embryonic development. It forms on the dorsal (back) face of the embryo, toward the caudal or posterior end.

Marginal zone: region corresponding to the equator between the two hemispheres in amphibian embryos.

Pair-rule genes: group of genes expressed in stripes during segmentation of the embryo in arthropods. In *Drosophila* pair-rule genes form seven dorsoventrally oriented stripes disposed along the antero-posterior axis.

Toll receptors: a class of single pass transmembrane receptors involved in patterning and immunity.

Planar Cell Polarity: the coordinated polarization of a field of cells within the plane of a cell sheet. The axis of planar polarity is typically orthogonal to that of the apico-basal polarity of epithelial cells.

Septins: Cytoskeletal components that upon binding to GTP can polymerize into ordered structures such as rings and filaments, which can function as scaffolds or diffusion barriers.

Advection: the transport of a substance or physical quantity by the movement of the surrounding environment.

Bandpass filter: a filter or a device that passes frequencies within a certain range and rejects frequencies outside that range.

Dissipation time scale: characteristic time at which the internal mechanical stress is reduced by a certain amount by viscous flow.

Epiblast (or primitive ectoderm): is one of two distinct layers arising from the inner cell mass in the mammalian blastocyst. The epiblast sits between the trophectoderm and the hypoblast (or primitive endoderm).

Primitive endoderm (or hypoblast): is the one of two layers arising from the inner cell mass in the mammalian blastocyst. The primitive endoderm sits between the epiblast and the blastocoel.

PVD neurons: sensory neurons responding to harsh touch and cold temperatures with a highly elaborate dendritic arborization in the nematode *C.elegans*.

Vpda class-I neurons: sensory neurons of the peripheral nervous system of *Drosophila* larvae. The classification is based on the morphology of the dendritic arborization with class-I being the simplest morphology and class-IV the most complex.

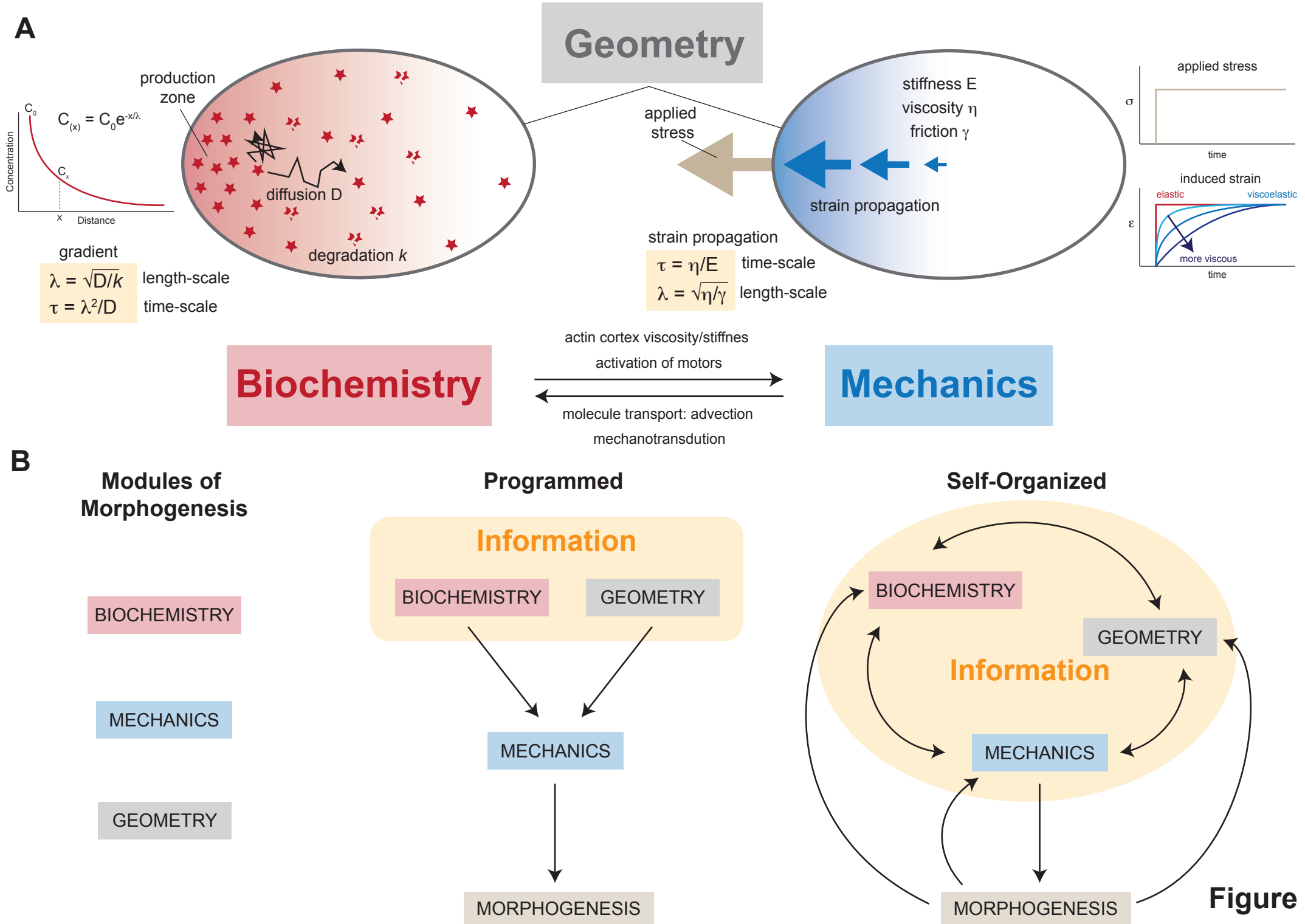
A
Geometry
production zone
$C_{(x)} = C_0 e^{-x/\lambda}$
Concentration
Distance
diffusion D
degradation k
gradient
$\lambda = \sqrt{D/k}$ length-scale
$\tau = \lambda^2/D$ time-scale
applied stress
stiffness E
viscosity η
friction γ
strain propagation
strain propagation
$\tau = \eta/E$ time-scale
$\lambda = \sqrt{\eta/\gamma}$ length-scale
applied stress
time
induced strain
elastic
viscoelastic
more viscous
time
Biochemistry
actin cortex viscosity/stiffnes
activation of motors
molecule transport: advection
mechanotransdution
Mechanics
B
Modules of Morphogenesis
BIOCHEMISTRY
MECHANICS
GEOMETRY
Programmed
Information
BIOCHEMISTRY
GEOMETRY
MECHANICS
MORPHOGENESIS
Self-Organized
BIOCHEMISTRY
GEOMETRY
Information
MECHANICS
MORPHOGENESIS

Figure 1

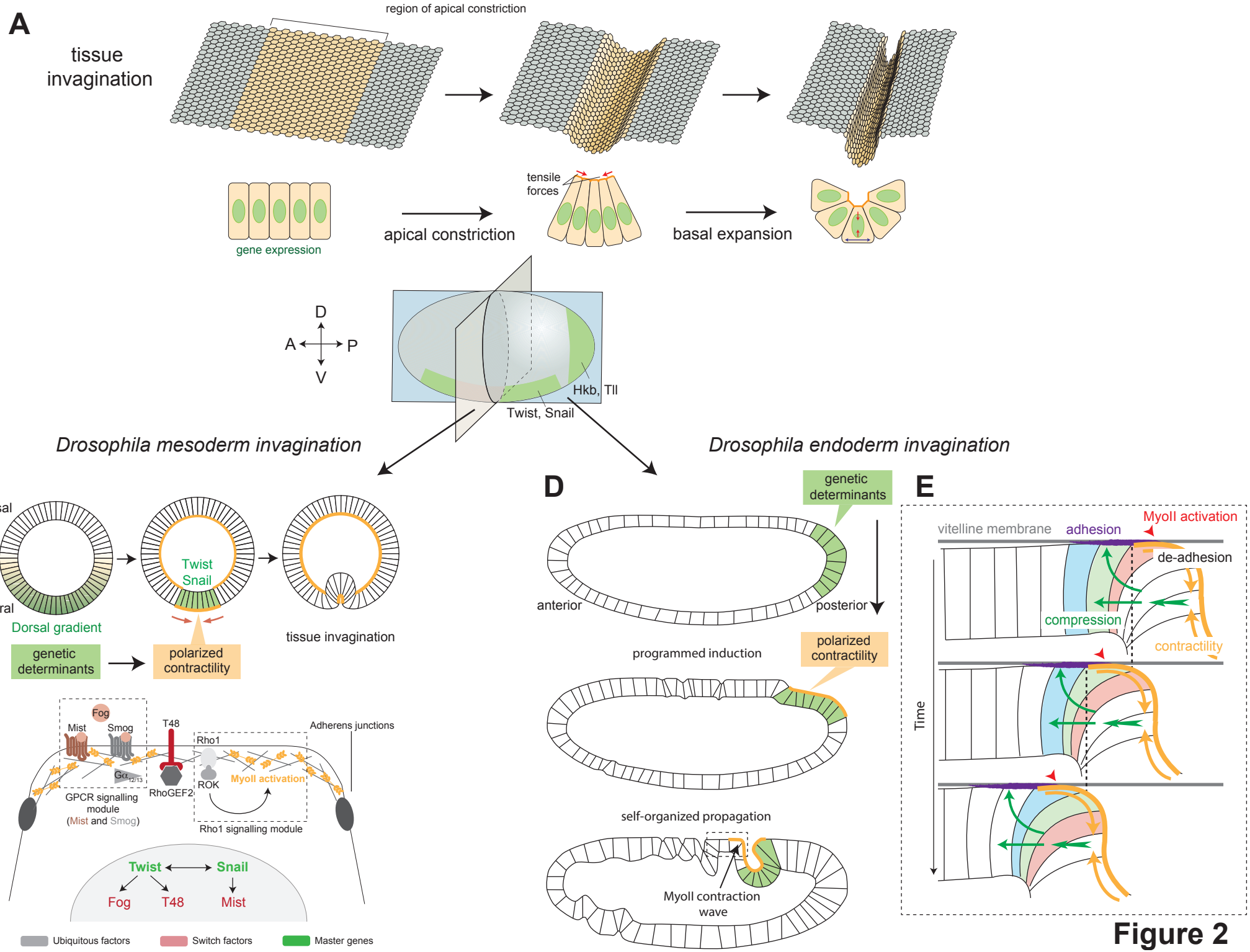
A
tissue invagination
region of apical constriction
gene expression
apical constriction
tensile forces
basal expansion
D
A
P
V
Hkb, Tll
Twist, Snail
Drosophila mesoderm invagination
Drosophila endoderm invagination
B
dorsal
ventral
Twist
Snail
Dorsal gradient
genetic determinants
polarized contractility
tissue invagination
C
Fog
Mist
Smog
T48
Rho1
Adherens junctions
Gα12/13
ROK
MyoII activation
RhoGEF2
GPCR signalling module (Mist and Smog)
Rho1 signalling module
Twist
Snail
Fog
T48
Mist
Ubiquitous factors
Switch factors
Master genes
D
genetic determinants
anterior
posterior
programmed induction
polarized contractility
self-organized propagation
MyoII contraction wave
E
vitelline membrane
adhesion
MyoII activation
de-adhesion
compression
contractility
Time

Figure 2

Figure 3

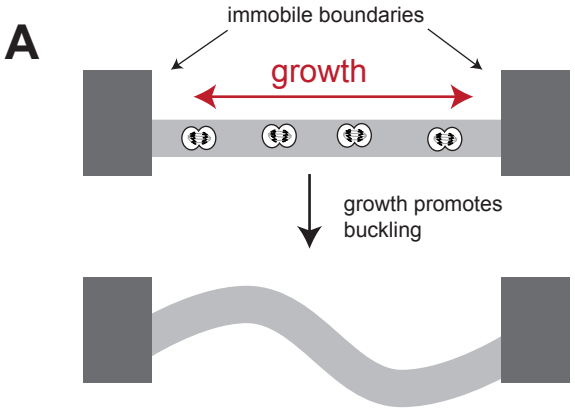

Brain cortex folding

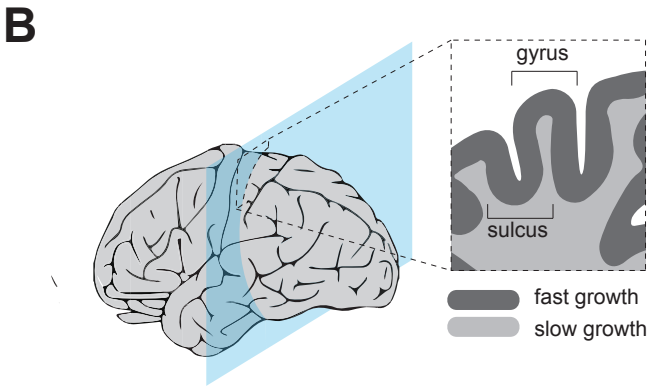

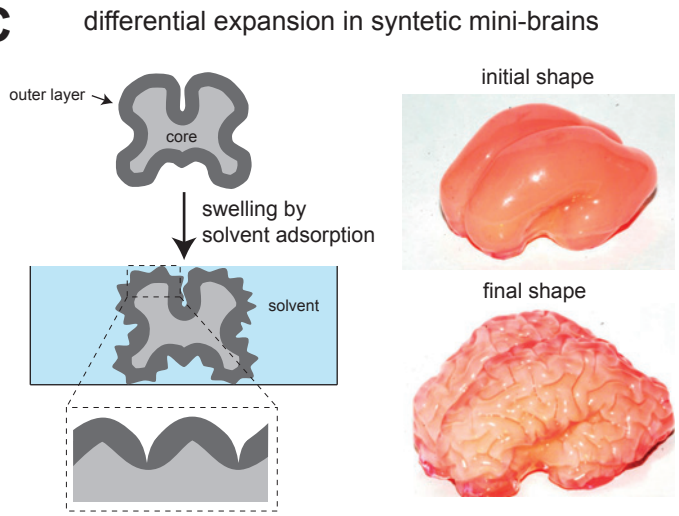

Gut morphogenesis

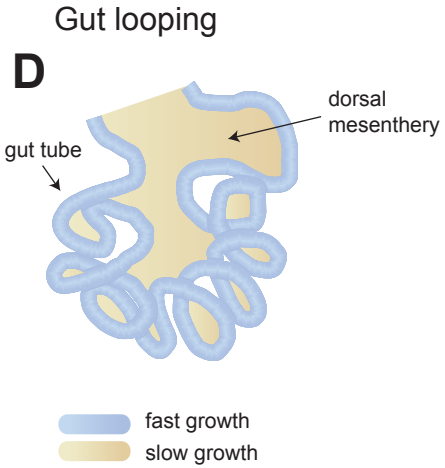

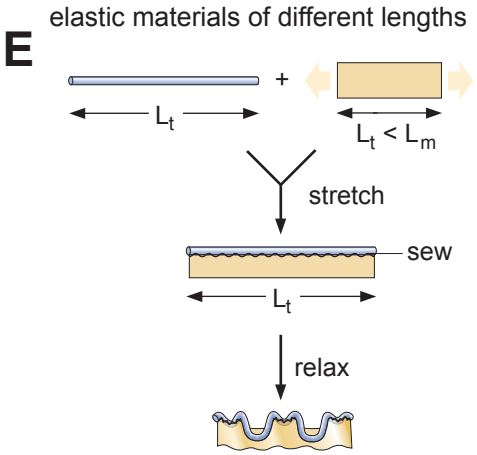

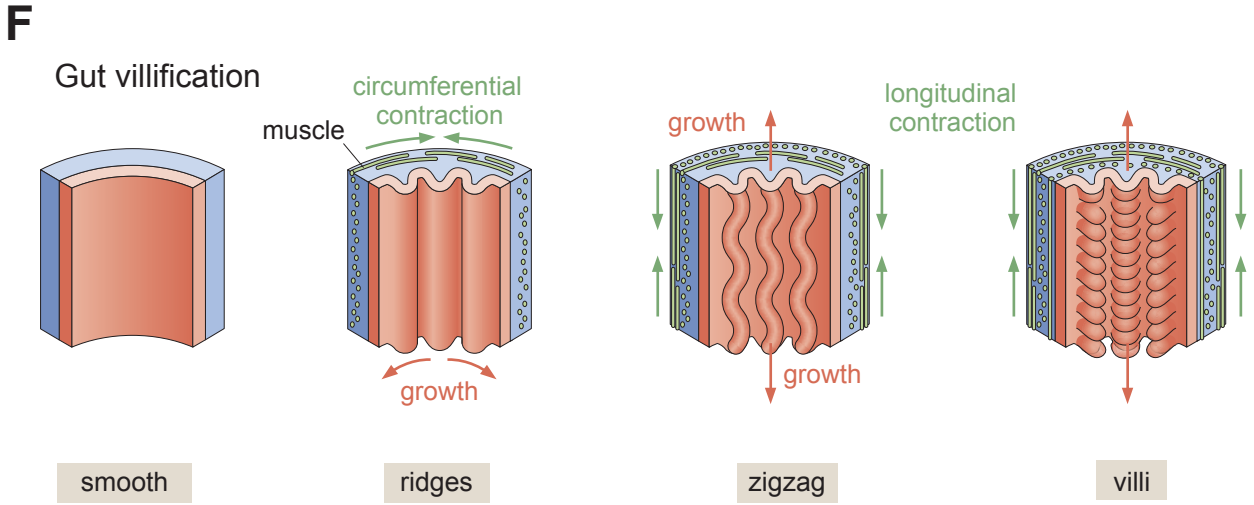

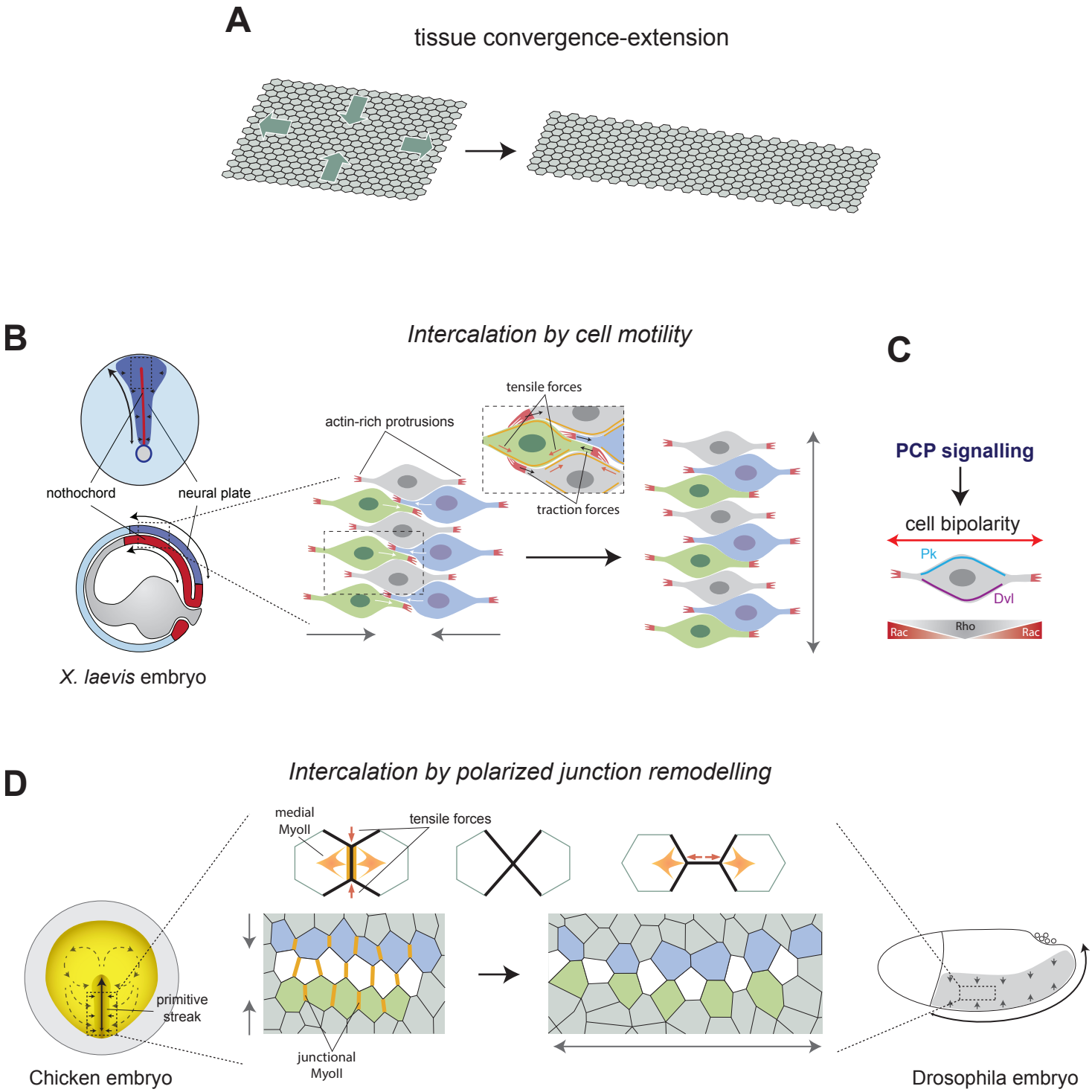
A
tissue convergence-extension
B
Intercalation by cell motility
nothochord
neural plate
X. laevis embryo
actin-rich protrusions
tensile forces
traction forces
C
PCP signalling
cell bipolarity
Pk
Dvl
Rac
Rho
Rac
D
Intercalation by polarized junction remodelling
medial
MyoII
tensile forces
primitive
streak
junctional
MyoII
Chicken embryo
Drosophila embryo
E
PCP signalling
Celsr1
Myosin II
cell bipolarity
Toll 2
Toll 8
Myosin II
2
6,8
2,6,8
2,8
6,8
6
2
Toll expression
Pair-rule genes
Anterior
Posterior
AP-patterning

Figure 4

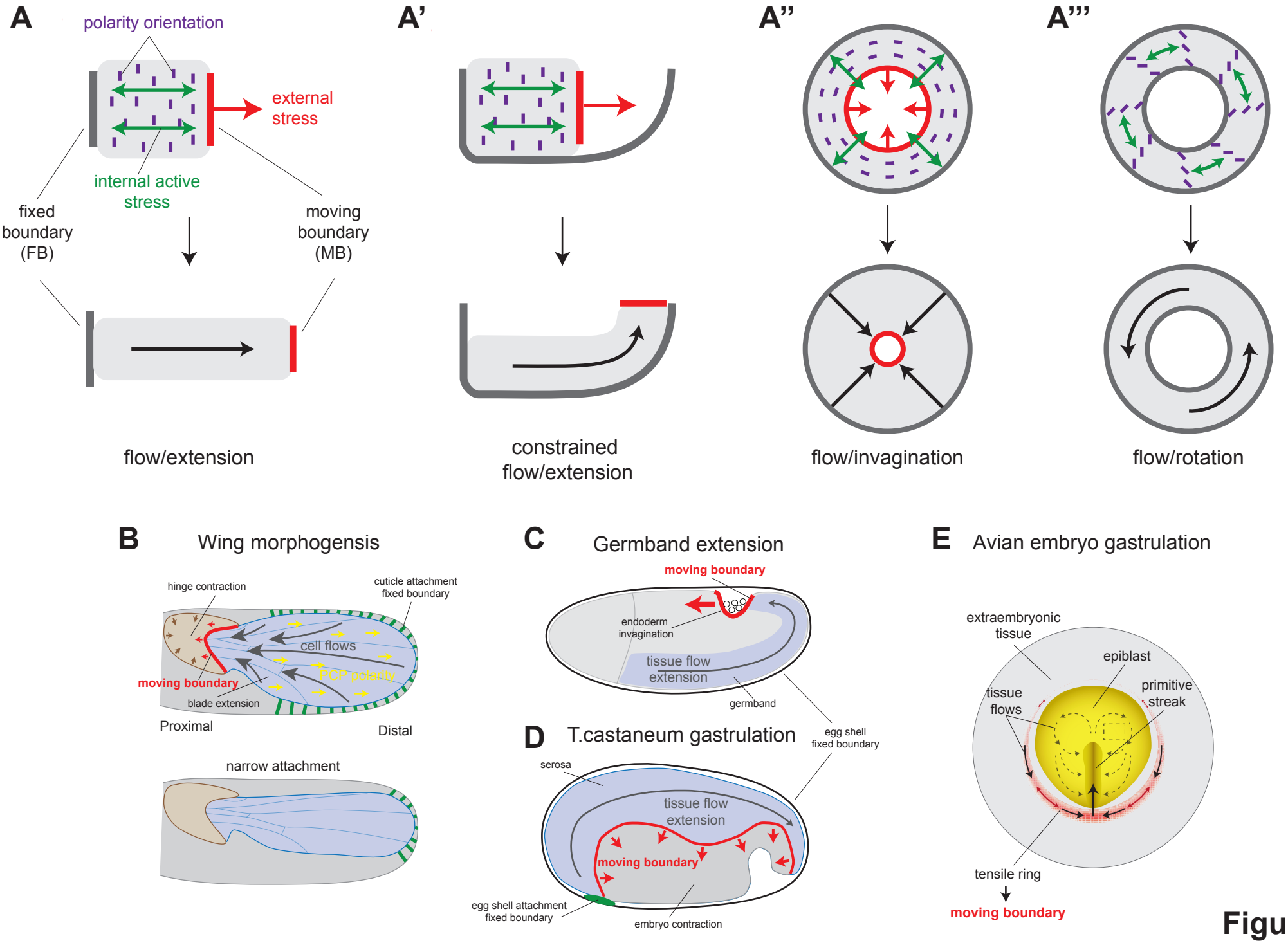
A
polarity orientation
external stress
internal active stress
fixed boundary (FB)
moving boundary (MB)
flow/extension
A'
constrained flow/extension
A''
flow/invagination
A'''
flow/rotation
B
Wing morphogensis
hinge contraction
cuticle attachment fixed boundary
cell flows
PCP polarity
moving boundary
blade extension
Proximal
Distal
narrow attachment
C
Germband extension
moving boundary
endoderm invagination
tissue flow extension
germband
egg shell fixed boundary
D
T.castaneum gastrulation
serosa
tissue flow extension
moving boundary
egg shell attachment fixed boundary
embryo contraction
E
Avian embryo gastrulation
extraembryonic tissue
epiblast
primitive streak
tissue flows
tensile ring
moving boundary

Figure 5

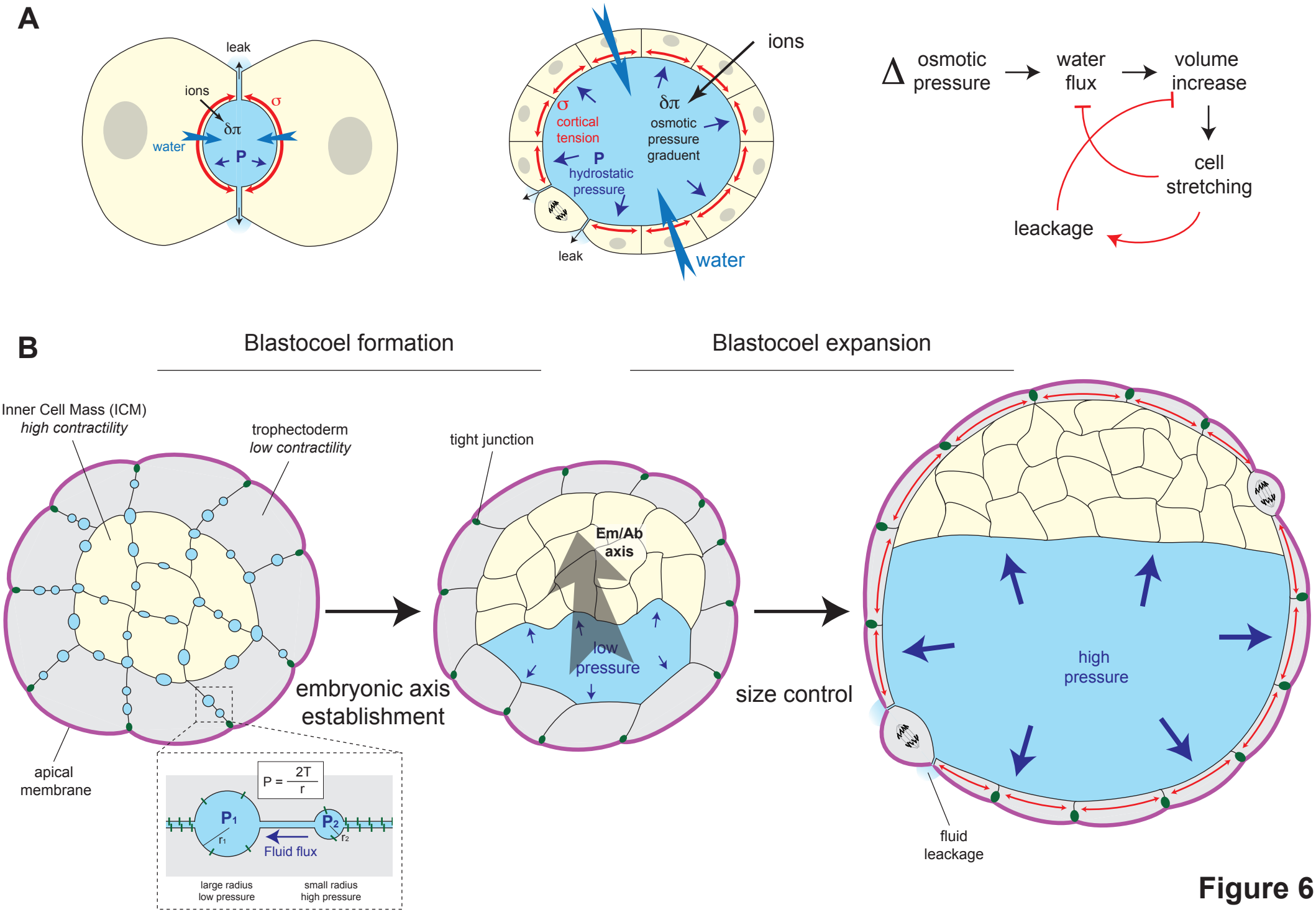
A
leak
ions
σ
δπ
water
P
ions
σ
cortical
tension
δπ
osmotic
pressure
graduent
P
hydrostatic
pressure
leak
water
Δ osmotic pressure
water flux
volume increase
cell stretching
leackage
B
Blastocoel formation
Blastocoel expansion
Inner Cell Mass (ICM)
high contractility
trophectoderm
low contractility
tight junction
Em/Ab axis
low pressure
high pressure
embryonic axis establishment
size control
apical membrane
P = 2T / r
P1
P2
r1
r2
Fluid flux
large radius
low pressure
small radius
high pressure
fluid leackage

Figure 6

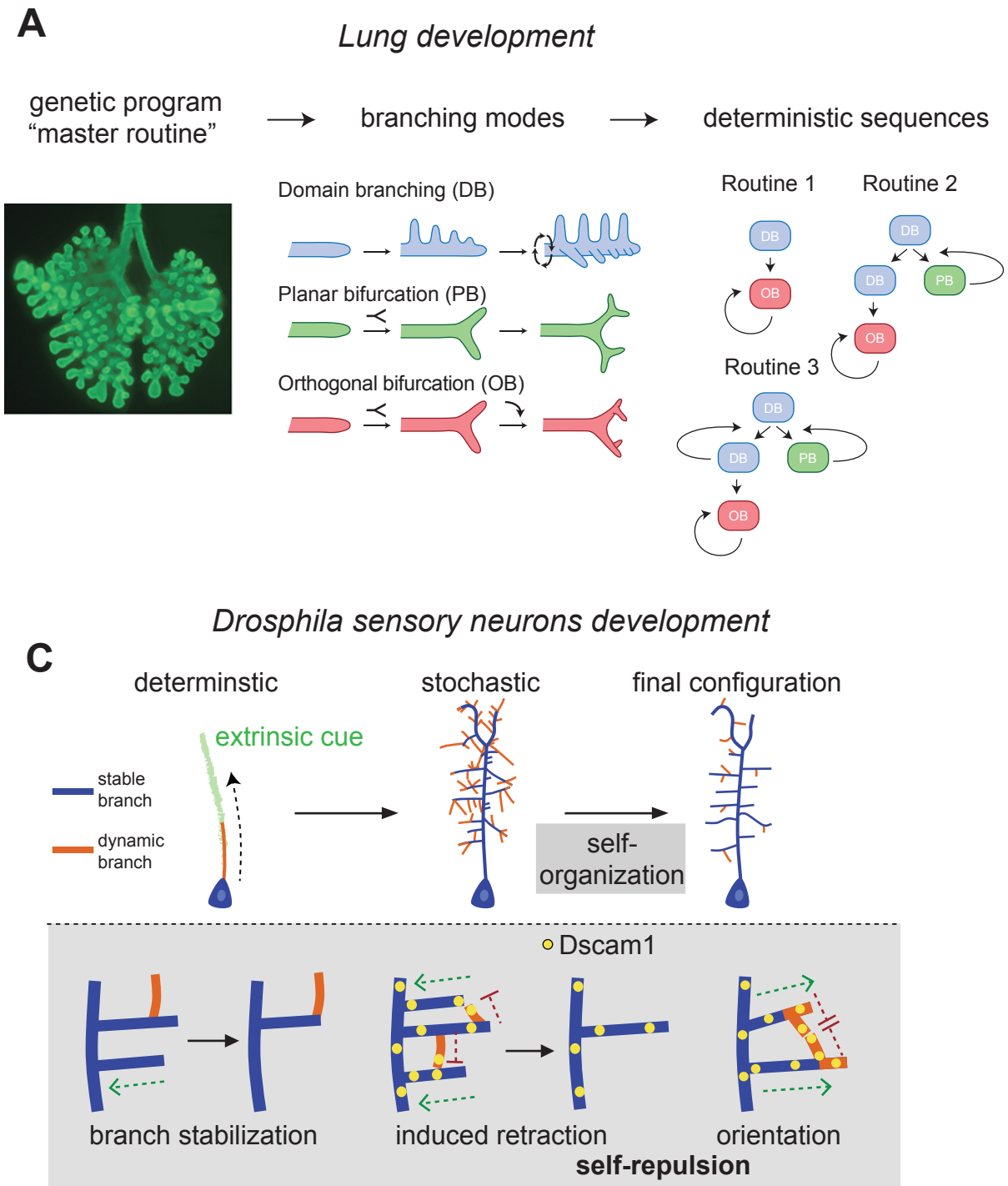
A
Lung development
genetic program
“master routine”
branching modes
deterministic sequences
Domain branching (DB)
Planar bifurcation (PB)
Orthogonal bifurcation (OB)
Routine 1
Routine 2
Routine 3
DB
OB
PB
B
Mammary gland development
stochastic tip behaviour
tip splitting
polarized growth
tip elongation
tip termination
active tips clustering
at growing front
constant branch density
C
Drosphila sensory neurons development
determinstic
stochastic
final configuration
extrinsic cue
stable
branch
dynamic
branch
self-
organization
Dscam1
branch stabilization
induced retraction
orientation
self-repulsion

Figure 7

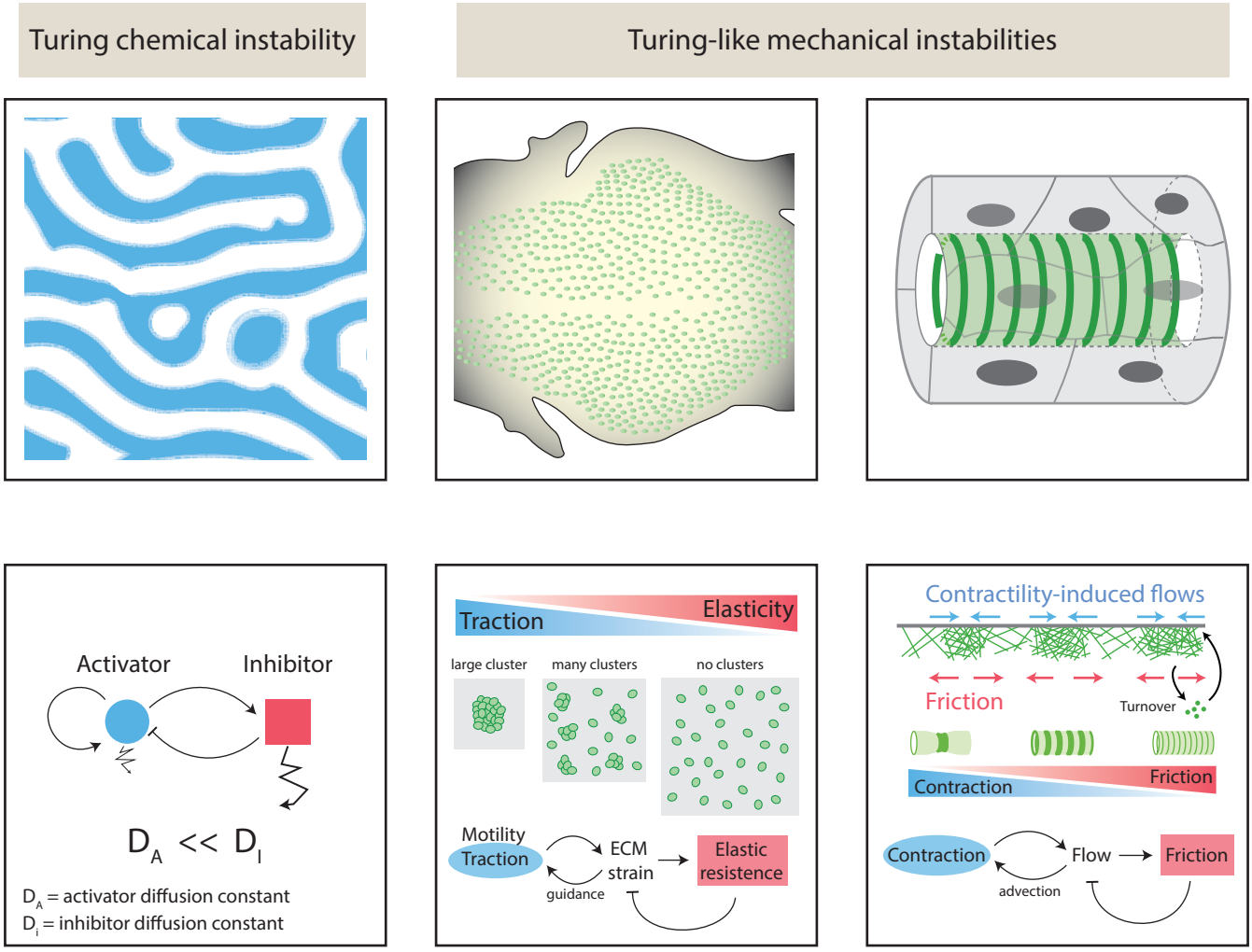
Turing chemical instability
Turing-like mechanical instabilities
Activator
Inhibitor
$D_A << D_I$
D_A = activator diffusion constant
D_i = inhibitor diffusion constant
Traction
Elasticity
large cluster
many clusters
no clusters
Motility
Traction
ECM
strain
guidance
Elastic
resistence
Contractility-induced flows
Friction
Turnover
Contraction
Friction
Contraction
Flow
Friction
advection
Local positive feedback - Long range inhibition

Figure Box2